From the Division of Radiology
Department of Clinical Science, Intervention and Technology
Karolinska Institutet, Stockholm, Sweden

BRAIN MRI AND CT MORPHOLOGY IN HEALTHY AGING AND ALZHEIMER´S DISEASE

Yi Zhang

Karolinska Institutet

Stockholm 2010

To

My Family

ABSTRACT

Background: The brain atrophy in individual Alzheimer's disease (AD) patients includes not only specific atrophy from AD pathology, but also atrophy induced by normal aging and cerebral vascular diseases. Although medial temporal lobe atrophy (MTA) together with CSF biomarkers is suggested to be the most important diagnostic markers for AD, it may not be specific. The current method of choice to measure MTA has been volumetric measurement based on 3D magnetic resonance imaging (MRI), but this complicated method has not been implemented clinically. Female sex has been suggested to be a risk factor for AD. The left hippocampus may be more vulnerable in AD. Atrophy of hippocampus has also been found to emerge in healthy adults, along with increased age.

Purposes: To investigate whether simple Computerized Tomography (CT) linear measurements of brain could be of value in AD work-up; to create a normative database of hippocampus volume in our large population-based study and to examine if there is an acceleration of hippocampal atrophy in normal aging; to examine the hippocampal and entorhinal cortex volumes in relation to vascular risk factors.

Material and Methods: In the CT study (Papers 1&2), 59 controls, 162 pure AD, and 86 AD with minor cerebrovascular changes (CVC) between the ages of 52 and 94 years were recruited from the Malmö Alzheimer Study. Abeta42, T-tau and P-tau in CSF were examined. CT linear measurements were performed, which included temporal horn ratio and suprasellar cistern ratio that reflect MTA. In the MRI study (Papers 3&4), 544 healthy non-demented subjects (aged 60-97 years) were recruited from the Swedish National study of Aging and Care in Kungsholmen (SNAC-K). Hippocampal formation and entorhinal cortex were manually delineated. Semi-automatic tools were used to access the volume of 3rd, lateral ventricle and intracranial volume (ICV). Vascular risk factors were collected.

Results: In the CT study (Papers 1&2), temporal horn ratio and suprasellar cistern ratio were the atrophy factors that contributed most significantly to the diagnoses with correct AD classification of 90.2%. The correct classification of AD+CVC from controls increased from 79.5% (only CSF biomarkers) to 84.6% (combined CT measurements with CSF biomarkers). However, little was changed in the pure AD group. In the MRI study (Papers 3&4), The normalized volumes of hippocampus in males were smaller than that in females. The right hippocampus was larger than the left. The rate of aging atrophy trend (AAT) for the expansion of ventricles was larger than the estimated hippocampal shrinkage. The age point (72y) was shown to represent the time when the acceleration of AAT in hippocampus starts in normal aging. The score of vascular risk factors was significantly associated with reduced volumes of hippocampus and entorhinal cortex only among men.

Conclusions: CT linear measurements could be of value in work-up of AD patients. Combined with the CT measure of MTA, the specificity of CSF biomarkers can be increased, but only in AD+CVC. In a non-demented elderly population, the females were more vulnerable to hippocampal atrophy. An acceleration of hippocampal atrophy may emerge and start around 72 years of age. An increasing burden of vascular risk factors is associated with reduced volume of hippocampus and entorhinal cortex.

Key words: Alzheimer disease, Brain, Atrophy, Diagnosis, CSF, CT, MRI, vascular risk factors, population-based study.

LIST OF PUBLICATIONS

I.   Zhang Y, Londos E, Minthon L, Wattmo C, Liu H, Aspelin P, Wahlund LO.
      Usefulness of computed tomography linear measurements in diagnosing
      Alzheimer's disease.
      Acta Radiol. 2008 Feb; 49(1):91-7.

II.   Zhang Y, Londos E, Minthon L, Wattmo C, Blennow K, Liu HJ, Bronge L,
      Aspelin P, Wahlund LO.
      Medial temporal lobe atrophy increases the specificity of cerebrospinal fluid
      biomarkers in Alzheimer disease with minor cerebrovascular changes.
      Acta Radiol. 2009 Jul; 50(6):674-81.

III. Zhang Y, Qiu C, Lindberg O, Bronge L, Aspelin P, Bäckman L, Fratiglioni L,
      Wahlund LO.
      **2009 IPA JUNIOR RESEARCH AWARDS – SECOND-PRIZE
      WINNER:** Acceleration of hippocampal atrophy in a non-demented elderly
      population, the SNAC-K study.
      Int Psychogeriatr. 2010 Feb; 22(1):14-25.

IV.   Qiu C*, Zhang Y*, Bronge L, Bäckman L, Fratiglioni L, Aspelin P,
      Wahlund LO.
      Cluster of vascular factors and hippocampal regional volumes among older
      adults: A population-based MRI study. *Manuscript*
      * sharing first author.

CONTENTS

LIST OF ABBREVIATIONS

AAT	Aging Atrophy Trend
AD	Alzheimer's Disease
AC	Anterior Commisure
ADAS	Alzheimer's Disease Assessment Scale
ANOVA	ANalysis Of VAriance
APOE4	Apolipoprotein E4 genotype
Aβ42	Amyloid Beta (1-42)
BMI	Body Mass Index
CI	Confidence Interval
CSF	Cerebral Spinal Fluid
CT	Computerized Tomography
CVC	Cerebrovascular Changes
DBM	Deformation-based Morphometry
DSM-IV-TR	Diagnostic and Statistical Manual of Mental Disorders, 4th edition Text Revision
DTI	Diffusion Tensor Imaging
ELISA	Enzyme-linked Immunosorbent Assay
FFS	Fast Field Echo
FLAIR	Fluid-attenuated Inversion Recovery
FOV	Field of View
FTD	Frontotemporal Dementia
ICC	Intraclass Correlation Coefficient
ICV	Intracranial Volume
MAb	Monoclonal Antibody
MANOVA	Multivariate ANalysis Of VAriance
MCI	Mild Cognitive Impairment
MMSE	Mini Mental State Examination
MPRAGE	Magnetization Prepared Rapid Acquisition Gradient Echo
MRI	Magnetic Resonance Imaging
MTA	Medial Temporal Lobe Atrophy
NINCDS-ADRDA	National Institute of Neurological and Communicative Disorders and Stroke and the Alzheimer's Disease and Related Disorders Association
OML	Orbitomeatal Line
PC	Posterior Commisure
PD	Photon Density
PET	Positron emission tomography
P-tau	Phosphorylated tau
P-tau181P	Phosphorylated tau at threonine 181
P-tau231P	Phosphorylated tau at threonine 231
ROI	Region of Interest
SE	Spin Echo
SNAC-K	Swedish National study of Aging and Care in Kungsholmen
SPSS	Statistical Package for the Social Sciences

TE	Time of Echo
TIA	Transient Ischemic Attack
TR	Time of Repetition
T-tau	Total tau
VBM	Voxel-based Morphometry

1 INTRODUCTION

1.1 ALZHEIMER'S DISEASE (AD)

Alzheimer's disease (AD) is a chronic progressive neurodegenerative disease and it is the most prevalent type of dementia [1].

AD is a large threat to public health in the 21st century [2]. Dementia doubles in frequency every 5 years after the age of 60, afflicting 1% of all 60-64 year olds and 30-40% of those aged 85 years and older [2, 3].

1.1.1 Clinical diagnosis

The NINCDS-ADRDA Alzheimer's Criteria were proposed in 1984 by the National Institute of Neurological and Communicative Disorders and Stroke and the Alzheimer's Disease and Related Disorders Association and are the most used in the diagnosis of AD [4] with good reliability and validity [5]. These criteria require the presence of cognitive impairment and that a suspected dementia syndrome should be confirmed by neuropsychological testing for a clinical diagnosis of possible or probable AD, at the same time as requiring histopathologic confirmation for the definitive diagnosis. They specify eight cognitive domains that may be impaired in AD: memory, language, perceptual skills, attention, constructive abilities, orientation, problem solving and functional abilities.

❖ **Definite Alzheimer's disease**: The patient meets the criteria for probable Alzheimer's disease and has histopathologic evidence of AD via autopsy or biopsy.
❖ **Probable Alzheimer's disease**: Dementia has been established by clinical and neuropsychological examination. Cognitive impairments also have to be progressive and be present in two or more areas of cognition. The onset of the deficits has been between the ages of 40 and 90 years and finally there must be an absence of other diseases capable of producing a dementia syndrome.
❖ **Possible Alzheimer's disease**: There is a dementia syndrome with an atypical onset, presentation or progression; and without a known etiology; but no co-morbid diseases capable of producing dementia are believed to be in the origin of it.
❖ **Unlikely Alzheimer's disease**: The patient presents a dementia syndrome with a sudden onset, focal neurologic signs, or seizures or gait disturbance early in the course of the illness.

Other commonly used criteria of Dementia of Alzheimer's Type are the DSM-IV-R criteria published by the American Psychiatric Association [6].
❖ The development of multiple cognitive deficits manifested by both, impaired memory, long or short-term, can't learn new information or can't recall information previously learned and is distinguished by:
  ♦ one (or more) of the following cognitive disturbances:
    • Aphasia (language disturbance).
    • Apraxia (impaired ability to carry out motor activities despite intact motor function).

- Agnosia (failure to recognize or identify objects despite intact sensory function).
- Disturbance in executive functioning (i.e., planning, organizing, sequencing, abstracting)

❖ The cognitive deficits above each cause significant impairment in social or occupational functioning and represent a significant decline from a previous level of functioning.

♦ The decline in mental functioning begins gradually and worsens steadily.
♦ The cognitive deficits above are not due to any of the following:
- Other central nervous system conditions that cause progressive deficits in memory and cognition (e.g., cerebrovascular disease, Parkinson's disease, Huntington's disease, subdural hematoma, normal-pressure hydrocephalus, brain tumor).
- Systemic conditions that are known to cause dementia (e.g., hypothyroidism, vitamin B-12 or folic acid deficiency, niacin deficiency, hypercalcemia, neurosyphilis, HIV infection).
- Substance-induced conditions.
♦ They aren't better explained by another Axis I disorder such as a Depressive Disorder or Schizophrenia.

The NINCDS-ADRDA and the DSM-IV-TR criteria for AD are the prevailing diagnostic standards in research; however, they have now fallen behind the unprecedented growth of scientific knowledge. Distinctive and reliable biomarkers of AD are now available through structural Magnetic Resonance Imaging (MRI), molecular neuroimaging with Positron emission tomography (PET), and cerebrospinal fluid analyses. They have led to proposals for revision of the NINCDS-ADRDA criteria that take these techniques into account [7]. These new criteria (called the Dubois criteria) are centred on a clinical core of early and significant episodic memory impairment. They stipulate that there must also be at least one or more abnormal biomarkers among structural neuroimaging with MRI, molecular neuroimaging with PET, and cerebrospinal fluid analysis of amyloid beta or tau proteins.

1.1.2 Complexity of diagnosis

At present, AD cannot be diagnosed until Alzheimer's dementia has been clinically established [8]. Moreover, in the earliest clinical stages of AD when symptoms are mild, clinical diagnosis can be difficult. The clinical "threshold value" varies greatly between individuals; it depends among other things on the patient's premorbid cognitive and intellectual level and is to some extent arbitrary. In clinically diagnosed populations, a higher level of specificity for biomarkers is difficult to achieve for methodological reasons, because even the gold standard, the clinical diagnostic criteria, cannot be absolutely specific [8].

Two diagnostic areas are especially challenging: firstly, differentiating early stages of Alzheimer's disease from mild cognitive impairment and normal aging; and

secondly, increasing diagnostic specificity especially when similar clinical symptoms are shared by various types of dementia [1].

A number of in vivo neurochemistry and neuroimaging techniques, which can reliably assess aspects of physiology, pathology, chemistry, and neuroanatomy, hold promise as biomarkers. Biomarkers can serve as early diagnostic indicators or as markers of preclinical pathologic change [8].

1.2 BRAIN ATROPHY

1.2.1 Brain atrophy in AD

Brain atrophy is an important anatomical change in the course of AD. In neuropathological studies, the end stages of AD are accompanied by a macroscopically detectable cortical atrophy, marked ventricular widening, and notable loss in brain mass [9]. Earlier MRI studies showed that structural changes such as medial temporal lobe atrophy (MTA) might serve as an indirect marker of AD and could be an early sign of AD [10-13]. This correlates significantly with the loss of cognitive functions [14].

Neurofibrillary pathology in AD typically emerges first in the entorhinal cortex and hippocampus [15-17] before spreading cortically to affect the rest of the temporal, parietal and frontal lobes [15, 17-22]. Decreased synaptic density and overt neuronal loss are evident on MRI as progressive cortical gray matter loss, reduced subcortical gray and white matter volumes, and expanding ventricular and sulcal cerebral spinal fluid (CSF) spaces [2, 23].

1.2.2 Medial temporal lobe atrophy (MTA) in AD

Neuronal loss of hippocampus and entorhinal cortex plays an important role in the development of MTA. The specificity of single MTA may not be enough to fulfill the proposed criteria for a new AD biomarker. Atrophy rates in longitudinal studies are only predictive under research conditions. They are not specific for AD and cannot be used as primary evidence for AD [24].

MTA is suggested to be a putative diagnostic marker for AD [25]. Most volumetric studies of Mild Cognitive Impairment (MCI) and AD patients have focused on the medial temporal lobe structures. One of the most important and most studied structures of the medial temporal lobe is hippocampus. Several studies have shown that patients with mild AD have about 25% smaller hippocampus than age matched controls [2, 26-28] whereas MCI patients show a reduction of around 11% [27]. Female sex has been suggested to be a risk factor for AD [29-31]. Left hippocampus may be more vulnerable in AD than right hippocampus due to smaller volume in the left [27, 32, 33]. It has also been suggested that small hippocampal volume at baseline may be associated with cognitive impairment and may predict decline to dementia [34, 35]. One population-based study found that reductions in hippocampal volume can be present before dementia but not until cognitive impairment is relatively severe [36]. To verify the development of MTA and hippocampus atrophy as diagnostic markers for AD, reliable and validated reference values for normal aging are needed. However, the majority of the studies on MTA and hippocampus atrophy are based on selected study populations. In order to obtain reliable and clinically useful reference values for hippocampus volumes in non-demented aged persons, a study based on a randomly selected population needs to be performed.

1.2.3   MTA in normal aging

As a part of the normal aging process, atrophy of hippocampus and other brain structures has also been found to emerge in healthy adults, in conjunction with increased age [37, 38]. Atrophy rate (%/y) was used to express the rate at which hippocampus size is reduced in percentage per year during a follow-up period. Adjusting for head size, an early study showed that the amygdala-hippocampus complex atrophied at a rate of 0.3% /year and the 3rd and lateral ventricles expanded 2.8% and 3.2%, respectively, in healthy volunteers (36-91 years old), but there was no gender difference of the atrophy rate [39]. However, two studies [40, 41] reported that the rate of hippocampus decline was greater in healthy males than in females. It has been reported that age-related hippocampal shrinkage starts in the mid-40s [41-45], which is in line with a study of brain weights based on over 20,000 autopsy cases [46]. Consistent with the longitudinal data, cross-sectional studies have documented smaller hippocampal volumes in middle-aged and old healthy males as compared to females [41, 47]. Few studies have reported a lateral asymmetry of hippocampus in healthy subjects, although many other brain structures have larger volumes on the right side as compared to the left [48].

1.2.4   Complexity of brain atrophy in Clinical diagnosed AD

It should be realized that most of the clinically diagnosed AD cases include not only MTA, but also other brain atrophy beyond normal aging. Besides normal aging and AD itself, minor cerebrovascular changes (CVC) in AD patients may change the patterns of the brain atrophy and neuronal damage.

Brain atrophy varies among individuals with clinically diagnosed AD. The brain atrophy in individual AD patients includes not only specific atrophy from AD pathology, but also atrophy induced by normal aging and cerebral vascular diseases [36].

1.3   CT IN AD

Computerized Tomography (CT) can be used to measure brain atrophy. It has been shown to be useful in some early AD studies [49]. Visual rating of CT images is widely used to study white matter changes reflecting vascular damage in AD [50, 51]. However, this has only been employed in very few atrophy studies of AD, since structural changes may not be reliably detected by visual inspection alone until the advanced stages of the disease [52, 53]. Planimetric area measurement is an objective tool used for estimating brain atrophy in CT [54, 55]. It has, however, seldom been used in AD, due to the lower resolution of the medial temporal lobe in CT.

1.4   LINEAR MEASUREMENTS

As a kind of traditional tool of anatomy in brain atrophy, linear measurements were further developed with the advent of CT. They have been widely used in CT to reliably evaluate brain atrophy [56, 57]. It does not measure volume directly, but by using a series of indices or ratios based on linear measurements, global and local brain atrophy, cortical and central atrophy can be assessed indirectly. Linear measurements are

simple, rapid and have a high reliability. The routine images of CT or MRI with thickness of 5 or 10 cm are usually enough for linear measurement.

1.5   3D HIGH-RESOLUTION MRI IN AD

3D high-resolution MRI images make it possible to more precisely measure volumes of brain structures, which is why MRI is the method of choice in evaluating MTA in AD [10, 21, 58].

A number of neuroimaging candidate markers are promising, such as hippocampus and entorhinal cortex volumes, basal forebrain nuclei, cortical thickness, deformation-based and voxel-based morphometry, structural and effective connectivity by using diffusion tensor imaging, tractography, and functional magnetic resonance imaging [8].

1.5.1   Manual tracing

Manual volumetric outlining using MRI images is time-consuming, and requires a highly skilled operator due to the anatomic variations of individual brain structures.

1.5.1.1   Hippocampus

High-resolution MRI determines structural changes in the brain in vivo. Significant atrophy of the hippocampal formation can be demonstrated by MRI even in preclinical stages of AD and predicts later conversion to AD with about 80% accuracy [59, 60]. Manual volumetric methods are currently the gold standard to determine the hippocampal volume [8].

Hippocampal volumetry is the best established structural biomarker for AD, particularly for early diagnosis. However, the procedure is still time-consuming and involves a great deal of manual work and therefore is not set to become a routine diagnostic test in the foreseeable future [8].

Several studies have focused on the temporal rate of change of hippocampal atrophy in AD patients. Atrophy rates of 3% to 7% per year were demonstrated [61, 62], whereas healthy controls showed a maximum atrophy rate of 0.9% in old age [44].

1.5.1.2   Entorhinal cortex

This area is hypothesized to be affected by the neurodegenerative process at a particularly early stage [8].

Studies have shown that entorhinal cortex volumetry is unlikely to provide any additional benefit to patients with manifest AD [33, 63-65].

1.5.2   Automatic volumetry

Automatic volumetry based on segmentation in MRI requires sophisticated software and high image quality, and the accuracy of the technique is yet to be established [52].

1.5.2.1   VBM

The most commonly investigated method to date is voxel-based volumetry (VBM) [66], which consistently shows a reduction in the cortical gray matter in the region of the mediotemporal lobes and lateral temporal and parietal association areas in AD

patients [67, 68]. However, VBM offers no direct way of making an individual diagnosis because it is always based on group statistics.

1.5.2.2 DBM

VBM transforms brain images into a standard space, thus compensating for global differences in the position of the head and the size of the brain and preserving local differences in the distribution of the cortical gray matter that can then be used as a basis for detecting group differences. Deformation-based morphometry (DBM) transforms the brain volumes at high resolution to a standard template brain, thus completely eliminating the anatomic differences between the brains. The anatomic information then is no longer found in the MRI images themselves but instead in the deformation fields that are required to transform the patient's brain into a standard brain. These deformation fields offer a multivariate vector field of localization information from which regional volume effects can be extrapolated. This method might thus be used for individual risk prediction [69].

1.5.2.3 Cortical thickness measurements

Another interesting automated method involves determining the cortical thickness of the neocortical association areas and the entorhinal cortex [70]. Group separation showed an accuracy of more than 90% in distinguishing between AD patients and healthy controls [71]. However, this method has yet to be evaluated in an independent group, and the accuracy of this method in predicting conversion to AD in MCI subjects has not yet been studied.

These drawbacks described above represent some of the reasons why these methods have not been fully clinically implemented. Therefore, it is necessary to find a more simple method to access atrophy in AD.

1.6 CSF BIOMARKERS

In the early stages of AD the use of specific CSF biomarkers may contribute to the diagnosis based on clinical and radiological approaches [72]. Decreased CSF amyloid beta (1-42) (Aβ42) is associated with intracerebral deposition of neuritic plaques, mainly composed of Aβ42. Increased CSF tau protein is considered to be a reflection of neuronal degeneration, caused by the intraneuronal accumulation of neurofibrillary tangles containing phosphorylated tau (P-tau). Measurements of total tau (T-tau) and Aβ42 in the CSF seem useful in discriminating early and incipient AD from age-associated memory-impairment, depression, and some secondary dementias [73]. CSF P-tau is increased in AD and may differentiate especially AD from other types of dementia. Although such CSF biomarkers provide reasonable accuracy and have already shown promise in aiding the diagnosis of AD [74], they may not be specific to AD [24, 72].

To date, the analysis of Aβ42, T-tau and P-tau from CSF are the best biological markers to diagnose Alzheimer's disease and to differentiate it from other forms of dementia with a high reliability and validity [1].

1.6.1 Aβ42

Amyloid beta (Aβ) peptide forms the main component of AD plaques primarily with a length of 42 amino acids (Aβ42) [75] and it is secreted by cells [76] showing a reduction of Aβ42 by about 50% in AD patients compared with nondemented controls of the same age. An autopsy study demonstrated an inverse correlation between Aβ42 levels in the CSF and the number of plaques [77]

1.6.2 T-tau

The main component relating to intraneuronal changes in AD patients is the microtubule-associated tau protein. Abnormal aggregates can only be formed if the tau protein is released from its sites of binding [78]. In AD patients, tau protein is present in a pathologic, hyperphosphorylated form. Tau protein was quantified in the CSF under the hypothesis that it is released extracellularly as a result of the neurodegenerative process. The methods initially available analyzed all forms of tau, regardless of their phosphorylation status at specific epitopes, i.e., total tau protein (t-tau) [8].

1.6.3 P-tau

Approximately 30 phosphorylation epitopes have been detected in AD. Most of these studies to date have investigated tau protein hyperphosphorylated at threonine 231 (p-tau231P) and at threonine 181 (p-tau181P). P-tau is promising in distinguishing AD from frontotemporal dementia (FTD), with sensitivity and specificity rates of 85% to 90% [78, 79]. CSF pathological measurements of p-tau and Aβ42 can assist in diagnosing vascular dementia or frontotemporal dementia in the differential diagnosis of AD indicated by a reasonable sensitivity and specificity [80].

1.7 CORRELATION BETWEEN CSF BIOMARKERS AND BRAIN ATROPHY IN AD

Both CSF biomarkers and MTA indicate cerebral degeneration and damage in AD. Relatively little is known about how they contribute individually to the diagnosis of AD and how they potentially correlate with each other. It was concluded in a study by Niki et al [81] that CSF biomarkers and MTA in MRI independently contribute to the diagnosis of AD, since there was no correlation between them. The combined use of MRI and CSF markers may present an incremental contribution to the early diagnosis of AD as well as help monitor the course of AD [24]. However, three other studies under various study conditions reported correlations between CSF markers with MTA, even with whole brain atrophy [24, 82, 83]. It is of interest to clarify the correlation between CSF biomarkers and brain atrophy and to explore the difference in their contribution to AD. It would then become possible to improve the specificity of AD diagnosis by CSF biomarkers and brain atrophy, and to correctly select tools to diagnose AD as well as to monitor the progress of AD.

1.8 VASCULAR RISK FACTORS AND BRAIN ATROPHY IN NORMAL ELDERLY

Recently, increasing evidence from magnetic resonance imaging (MRI) studies has emerged that, among older adults, vascular risk factors and diseases may contribute to the age-associated changes in the brain structure [84, 85], which may result in cognitive dysfunction in a non-demented population [84].

2 PURPOSES

2.1 PAPER 1

Considering the inexpensiveness and high availability of CT as well as the simplicity of linear measurement, we applied a series of linear measurements in CT to investigate their value in evaluating brain atrophy in the work-up procedure of AD patients. This is of particular importance since a brain scan has been strongly recommended in the initial dementia work-up to exclude hydrocephalus, subdural collections, and brain tumors. Therefore, the linear measurements that most significantly reflect atrophy of AD patients were examined and their contributions to the diagnosis in combination with other clinical examinations were studied.

2.2 PAPER 2

A previous study (9) of CT linear measurements in AD has shown that two of the measurements (temporal horn ratio and suprasellar cistern ratio), which most reflect MTA and also partially reflect central atrophy, can discriminate AD from healthy elderly controls. The aim of this study was to further investigate the validity of the radiological linear measurements of brain atrophy in AD diagnosis. This was done by examining the correlation with the CSF biomarkers and by examining if the specificity could be improved in classification of AD from controls, when the linear measurements are combined with the CSF biomarkers.

2.3 PAPER 3

The aim of the study is two-fold. In order to implement MTA and hippocampus atrophy as a diagnostic marker for AD, more reliable data on normal hippocampus volume obtained from a large population-based study is needed. The first aim, therefore, is to create a normative database of hippocampus volume in different age cohorts (60-90+), and study gender differences and the lateral asymmetry as compared with the lateral and 3rd ventricle in a large population-based study. Moreover, few studies have been undertaken to investigate the acceleration of hippocampal atrophy in normal aging, including at what age does an acceleration of hippocampal atrophy start in non-demented elderly. Accordingly, the second aim is to study the aging atrophy trend in normal aging (AAT is used to express the speed and acceleration of brain atrophy that is the atrophy trend in a cross-sectional volume database, rather than atrophy rate as used in longitudinal data).

2.4 PAPER 4

Few studies so far have investigated the influence of vascular factors and cluster of multiple vascular factors on brain structure, especially with regard to the medial temporal lobe such as hippocampus and entorhinal cortex. Based on MRI image analysis, we quantified brain tissue volumes of these two regions on a population-based sample of older adults. We sought to investigate whether and to what extent these regional volumes were affected by cardiovascular risk factors. It is hypothesized that vascular factors and aggregation of multiple vascular factors in particular, may exert a detractive effect on medial temporal lobe area of the brain.

3 MATERIAL AND METHODS

3.1 MATERIAL

3.1.1 Subjects 1 (papers 1&2)

Fifty-nine healthy controls and 248 dementia patients (162 AD, 86 AD with cerebrovascular changes (AD+CVC)) with an age range of 52-94 years were recruited from a cross-sectional study, the Malmö Alzheimer Study. All patients were investigated at the Neuropsychiatric Clinic, Malmö University Hospital, Malmö, Sweden and were evaluated using a detailed clinical investigation including cognitive function from 1999 to 2003. Only AD patients with mild or moderate disease together with a complete investigation including brain CT were selected to participate in the study.

The controls (n=59) were recruited through advertisements. Only individuals with neither subjective memory problems nor CVC were selected. Volunteers underwent the same physical examinations, cognitive testing and brain CT. The inclusion criteria were a Mini Mental State Examination (MMSE) [86] test result of 28 or above and an Alzheimer's Disease Assessment Scale (ADAS-cog) [87] test result of 12 or below. The exclusion criteria were mild cognitive impairment (MCI), dementia or other mental or physical illness, which could affect the cognitive status.

This study was approved by the ethics committee of Lund University, and informed consents were obtained from all participants.

3.1.2 Processing of subjects 1

The diagnostic criteria used were NINCDS-ADRDA for probable Alzheimer's disease [4]. In addition we sub-grouped the AD patients into "pure AD" and "AD with minor cerebrovascular changes" (AD+CVC) in order to clarify the possible influence on atrophy from cerebrovascular changes in AD patients. AD+CVC was defined as AD subjects with signs of cerebrovascular disease (leuko-araiosis and/or minor infarctions on CT, or a history of minor stroke/transient ischemic attack (TIA). No clinical relation between the cerebrovascular incident and cognitive decline was identified. Consequently, cerebrovascular changes were not severe enough to fulfill the NINDS-AIREN criteria of vascular dementia. A complete investigation included medical history, physical and neuropsychiatric examination, tests of cognitive function, blood sampling, including apolipoprotein E4 genotype, CSF and brain CT. The cognitive status of the patients was evaluated using MMSE and ADAS-cog. The neuropsychiatric state was evaluated by collecting data of behavioral and psychological symptoms in dementia.

3.1.3 Subjects 2 (paper 3&4)

Five hundred and fifty-two subjects were recruited into the MRI study by using a sub-sample of an epidemiological sample of 3363 healthy non-demented elderly population (over 60 years old) who are participating in the Swedish National study of Aging and Care in Kungsholmen (SNAC-K). This longitudinal and multidisciplinary study of aging and health began in 2001. SNAC-K was designed to detect the influence of lifetime genetic, environmental, and biological factors on medical, psychological and social health in late adulthood. The SNAC-K samples were stratified for age cohort and

year of assessment. Eleven age cohorts were chosen with different assessments intervals: six years in the younger cohorts (60-78 years old), and three years in the older cohorts (age 78+). The follow-up intervals were determined in order to balance the more rapid changes and higher attrition in the older cohort. The baseline data collection includes information on present status and past events. The information has been collected through interviews, clinical examinations, and testing. The baseline data collection was completed in June 2004 and the follow-up data collection is ongoing. During the baseline SNAC-K examination, among all non-institutionalized and non-disabled participants, 552 subjects were randomly selected to undergo a MRI examination. On average, these subjects were slightly younger, more educated, and cognitively advantaged compared to the remaining sample. Subjects with severe cerebral diseases that directly affect brain atrophy were excluded. Following a quality assessment of the baseline MRI images, 544 subjects (aged 60-97 years old, 318 females, and 226 males) were finally included in the MRI study at baseline. Due to the small sample size in the groups 87 years and 87+ years, these groups were combined into one group. Thus, a total of seven age groups (60, 66, 72, 78, 81, 84, and 87+ years) were used in the study.

3.1.4 Processing of subjects 2

Participants were invited to the aging research center to respond to the structured questionnaire surveys carried out by the center's trained nurses and for the clinical examination carried out by its physicians. If the subjects were not willing or not able to come to the research center, home visits by nurses and physicians were arranged. Global cognitive function was evaluated with MMSE. The questionnaire surveys collected information on demographic features (i.e., age, gender, and education), health history (e.g., hypertension, diabetes, and coronary heart disease), lifestyles and habits (e.g., cigarette smoking, alcohol consumption, and physical activity), and use of medical drugs (e.g., blood pressure lowering and blood glucose lowering drugs). Education was measured by the maximum years of formal schooling. Weight and height were measured in light clothes without shoes, and body mass index (BMI) was calculated as measured weight (kg) divided by height squared (m^2). Smoking was categorized into current, former, and never smoking, alcohol consumption was classified into binge drinking ($\geq$5 drinks on one occasion and at least once a month), non-binge drinking, and not drinking or less than once a month. Physical activity was categorized into daily-to-weekly, less than weekly-to-monthly, and no regular physical activity. Because most people (91.4%) had some kind of light activity (e.g., short walks and light gym), only intensive physical activity (e.g., jogging, brisk long-walks, and long cycling) was analyzed. Arterial blood pressure (i.e., systolic Korotkoff phase I and diastolic phase V) was measured twice, in the sitting position, on the right arm with a random-zero sphygmomanometer, each with at least a 5-minute interval. The mean of the two readings was used in defining hypertension. Hypertension was considered to be present if subjects had systolic pressure $\geq$160 mm Hg, or diastolic pressure $\geq$90 mm Hg, or currently took blood pressure lowering drugs (Anatomical Therapeutic Chemical classification system codes: C02, C03, C07, and C08). Diabetes mellitus was defined as having self-reported history of diabetes or use of oral blood glucose lowering drugs or insulin. Total cholesterol level was measured following the standard procedure, and high total cholesterol was defined as $\geq$6.5 mmol/L.

3.2 METHODS OF CSF BIOMARKERS

CSF was collected by lumbar puncture in polypropylene tubes, gently mixed to avoid gradient effects, centrifuged at 2000×g for 10 min, and aliquots were stored at −80 °C pending biochemical analysis. T-tau was determined using a sandwich enzyme-linked immunosorbent assay (ELISA) constructed to measure T-tau (both normal tau and P-tau) [88]. P-tau (P-Thr181) was determined using a sandwich ELISA, with monoclonal antibody (MAb) HT7 (recognizing all forms of tau) used as capturing antibody and biotinylated MAb AT270 (specific to P-Thr181 P-tau) used as a detection antibody [89]. Aβ42 was determined using a sandwich ELISA specific for Aβ42, as previously described [90].

3.3 NEUROIMAGING METHODS

3.3.1 CT acquisition

All subjects underwent non-contrast cranial CT using the Somatom Plus 4 scanner (Siemens, Erlangen, Germany). Scanning utilized the following parameters: 140KV, 306mAs in the posterior fossa and 309 mAs in supratentorial brain. Axial images with 5mm slice thickness were taken parallel to the orbitomeatal line (OML).

3.3.2 CT Linear measurements

Linear CT measurements were obtained directly from films. The rater (Y.Z) was blinded for clinical data regarding the subjects. The following linear measurements were performed using digital caliper (Mitutoyo®) (Fig. P1-1a, 1b, 1c): maximal transversal intracranial width (A), maximal longitudinal intracranial width (B), maximal width of frontal skull (C), maximal frontal horns width (E), minimal intercaudate distance (F), minimal ventricular bodies width (G), maximal width of 3rd ventricle (H), maximal width of frontal subarachnoid space (I), the distance between the choroid plexuses (J), the sum of widths of the four widest sulci (M), width of cistern ambiens (N), temporal horn diameter (O) and suprasellar cistern width (P). The following combined indices and ratios were calculated from these measurements: Evans ratio (E/C), bicaudate ratio (F/A), Huckman number (E+F), cella media index (G/A), 3rd ventricular ratio (H/A), ventricle index (J/E), frontal subarachnoid ratio (I/B), four cortical sulci ratio (M/A), cistern ambiens ratio (N/A), temporal horn ratio (O/A), suprasellar cistern ratio (P/A) [56, 91-96].

Fig. P1-1a

Fig. P1-1b

13
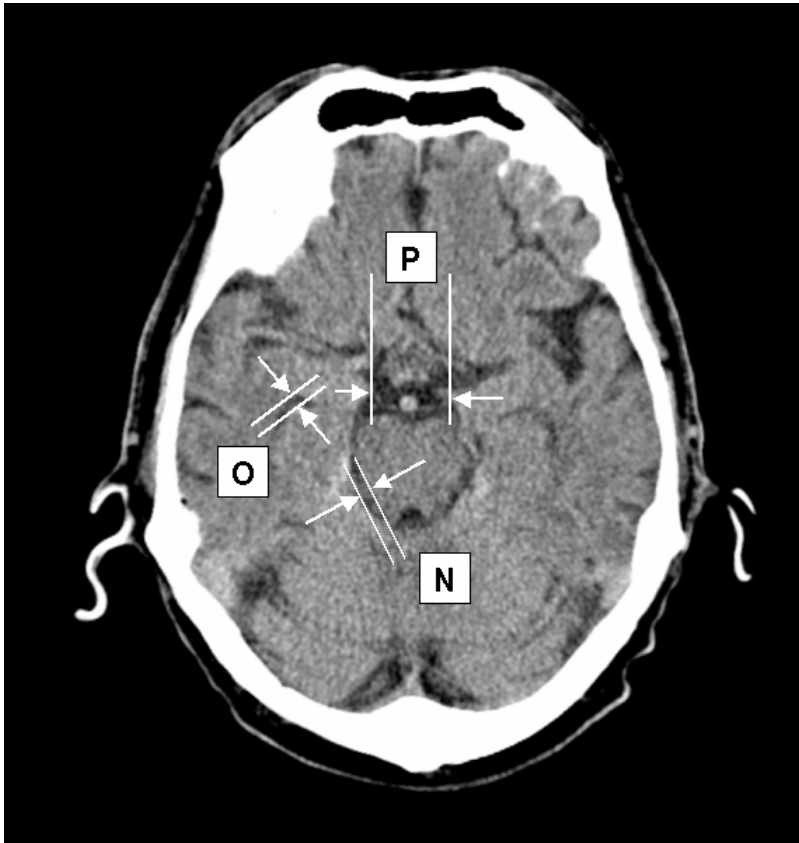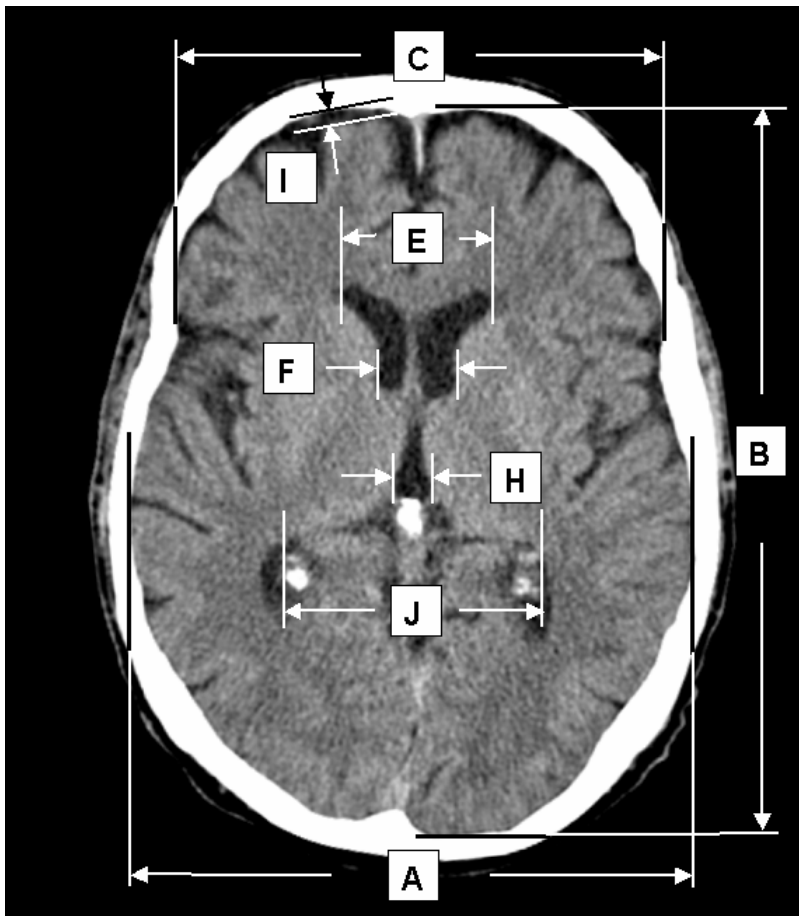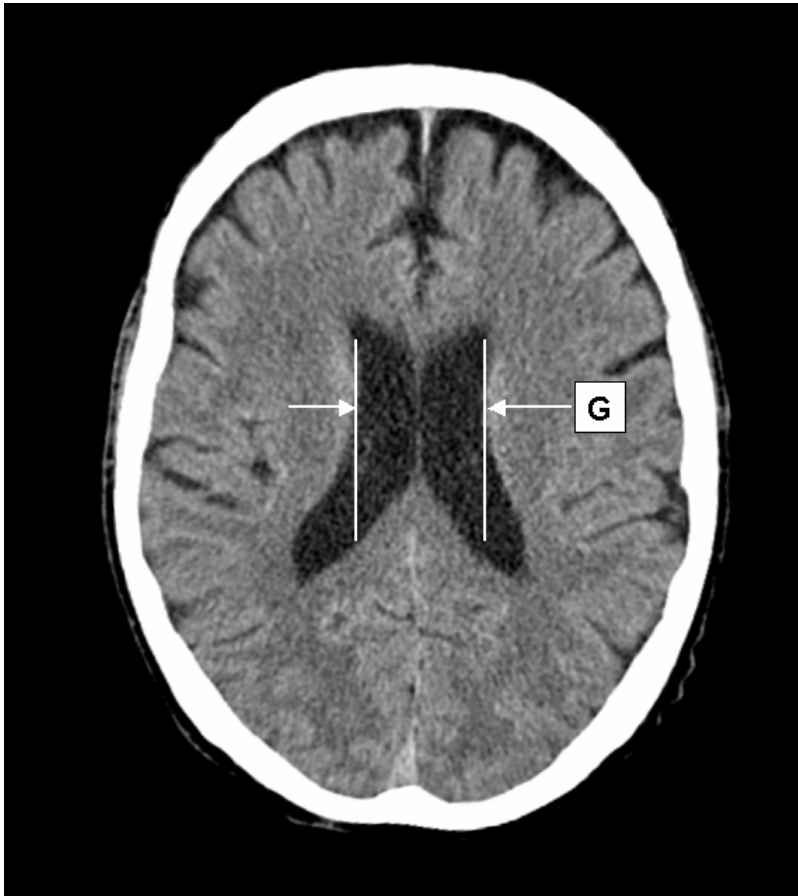
Fig. P1-1c

3.3.3 Reliability of CT linear measurements

Intra-rater reliability for each measurement was assessed by comparing repeated measurements from fifteen subjects selected randomly. The interval between the repeated measurements was four weeks. The intraclass correlation coefficient (ICC) ranged from 0.95 to 0.99, with the exception of 0.84 for the four cortical sulci ratio (M/A) and 0.90 for the frontal subarachnoid ratio (I/B) (Table P1-1).

Table P1-1. Intra-rater reliability of the CT linear measurements by intraclass correlation coefficient (ICC)	
	ICC
Maximal transversal intracranial width (A)	0.97
Maximal longitudinal intracranial width (B)	0.98
Maximal width of frontal skull (C)	0.98
Evans ratio (E/C)	0.97
Bicaudate ratio (F/A)	0.98
Huckman number (E+F)	0.98
Cella media index (G/A)	0.98
3rd ventricular ratio (H/A)	0.98
Ventricle index (J/E)	0.97
Frontal subarachnoid ratio (I/B)*	0.9
Four cortical sulci ratio (M/A)*	0.84
Cistern ambiens ratio (N/A)	0.95
Temporal horn ratio (O/A)	0.99
Suprasellar cistern ratio (P/A)	0.98
* The linear measurements of lower intra-rater reliability are marked.	

3.3.4 MRI acquisition

MRI scanning was undertaken on a 1.5T scanner (Philips Intera, Netherlands). 3D FFE (Fast Field Echo) T1, Axial SE (Spin Echo) PD (Proton Density) /T2, Axial FLAIR (Fluid-attenuated Inversion Recovery) and Axial DTI (Diffusion Tensor Imaging) were acquired. In this study, the 3D FFE T1 images (TR (Repetition Time) = 15ms, TE (Echo Time) = 7ms, Flip angle = 5°, Number of slices = 128, Thickness = 1.5mm, FOV (Field of View) = 240, Matrix = 256*256) were used for volumetry.

3.3.5 MRI Image processing

Images were transferred to a HERMES workstation (Nuclear Diagnostics, Stockholm, Sweden), where each of the volumetric measurements was performed with constant parameters by Y.Z, who was blinded to clinical information. This was done to maximize uniformity in image processing and measurement. The transversal 3D FFE images were reoriented to coronal sections orthogonal to AC-PC (anterior commisure to posterior commisure) line. STEREOLOGY [97], a volumetric software in HERMES, was used to acquire intracranial volume (ICV). This is an accurate semi-automatic method for estimating large brain structures that are too time-consuming to be delineated directly. Using the MultiModality ROI tool in HERMES, the hippocampal formation was manually delineated. Another semi-automatic tool of Region Growing in HERMES MultiModality was used to measure lateral and 3rd ventricles. Due to individual variations of signal intensity distribution, a test of the growing effect by visual checking was done to set specific individual parameters before each final growing volume was produced. When "leakage" of ROI occurred after growing, manual masking before growing was performed.

3.3.6 Volumetric measurements:

Intra-rater reliability of the measurements was tested in 15 randomly selected subjects by repeated measurements with an interval of one month. ICC of the measurements was > 0.93.

3.3.6.1 Hippocampus formation

A previously used protocol [98], which was focused on anatomic accuracy, was slightly modified to delineate the hippocampal formation. It was defined to include the grey matter (hippocampal proper (cornu ammonis regions; Ammon´s horn), the dentate gyrus, the subiculum) and some white matter (alveus, fimbria). Parahippocampal gyrus, entorhinal cortex, and fornix were excluded. One advantage of the protocol is that it includes the full tail of the hippocampus. Since the anterior limit of hippocampus in the original protocol was hard to identify in some brains, we modified it as specified below. To find the posterior limit, the slice where the fornix is most clearly seen in the coronal plane was determined, and the grey matter of the hippocampus was followed through posterior slices until no more grey matter is seen. Measurement starts at this location, which is the hippocampal tail that extends into the grey matter that protrudes into the triangle of the lateral ventricle, ventral to the splenium of the corpus callosum. The lateral border was defined by the temporal horn of the lateral ventricle and/or white matter adjacent to the hippocampal grey matter. The inferior border is demarcated by the white matter of parahippocampal gyrus. For the superior boundary, the alveus was included where it overlays the hippocampus, excluding the pulvinar. For the mesial boundary on the posterior slices, the natural border of the gray matter was followed. On more anterior slices, the uncal notch was determined and the measurement was made straight up from there, forming the mesial boundary. The anterior border was complicated by the presence of the amygdala. The signal intensity difference between hippocampus and amygdala was used to identify the border, instead of anatomical markers. (Fig. P3-1)

16
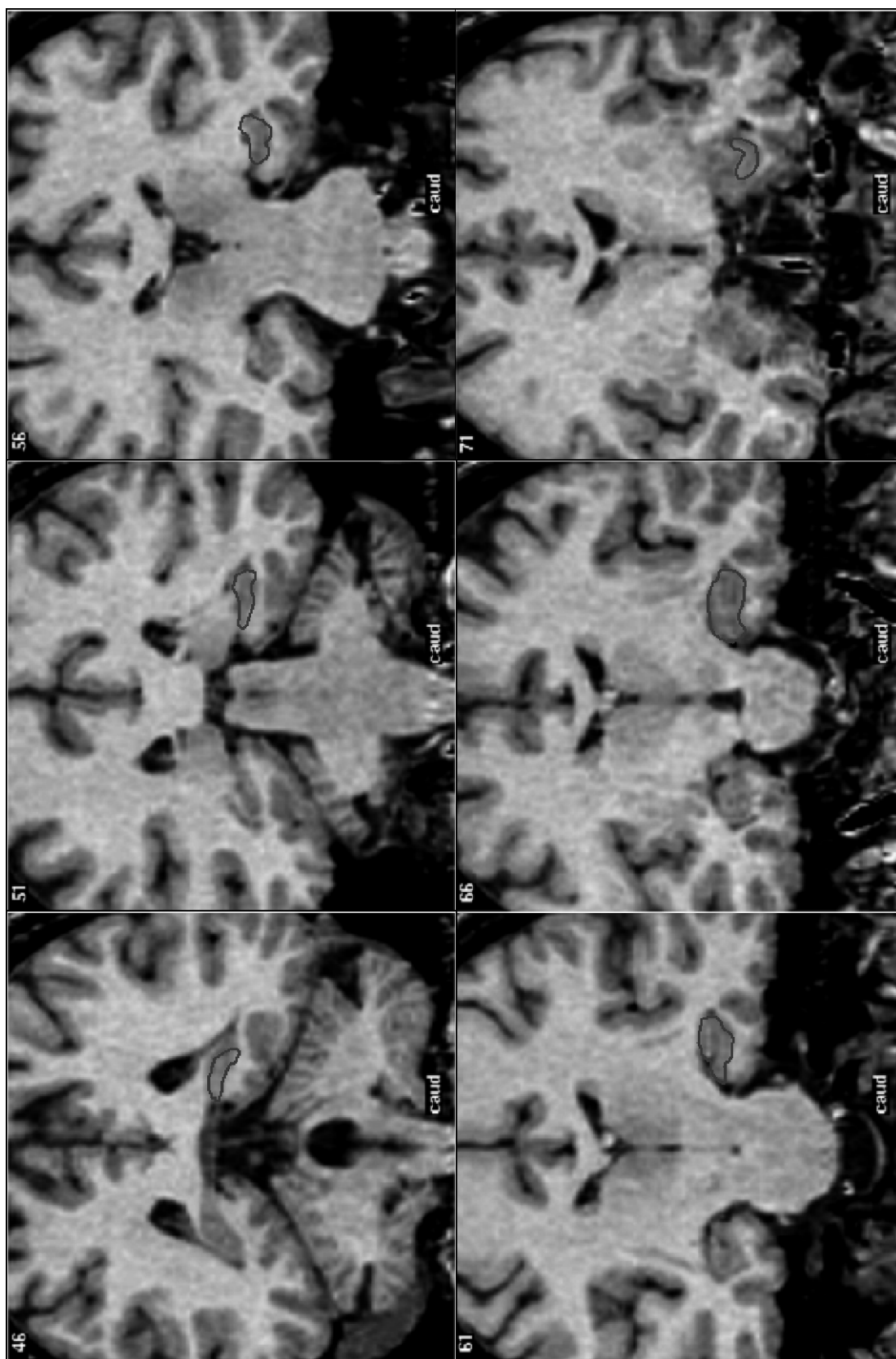
Fig. P3-1

3.3.6.2 Entorhinal cortex

Using a modified protocol based on the previous protocols [99, 100], EC was also manually traced in coronal slices using a 2.0 zoom factor. The anterior boundary of EC was the presence of sulcus semiannularis. If the sulcus was not visible, it was defined as the second slice behind temporal stem. The landmark of posterior boundary was the end of the gyrus intralimbicus. The supero-medial boundary of EC was where the white matter was separated from the amygdala (rostrally) and hippocampus (caudally). The natural shape of grey matter on the medial side of collateral sulcus was used as the infero-lateral boundary of entorhinal cortex. (Fig. P4-1)
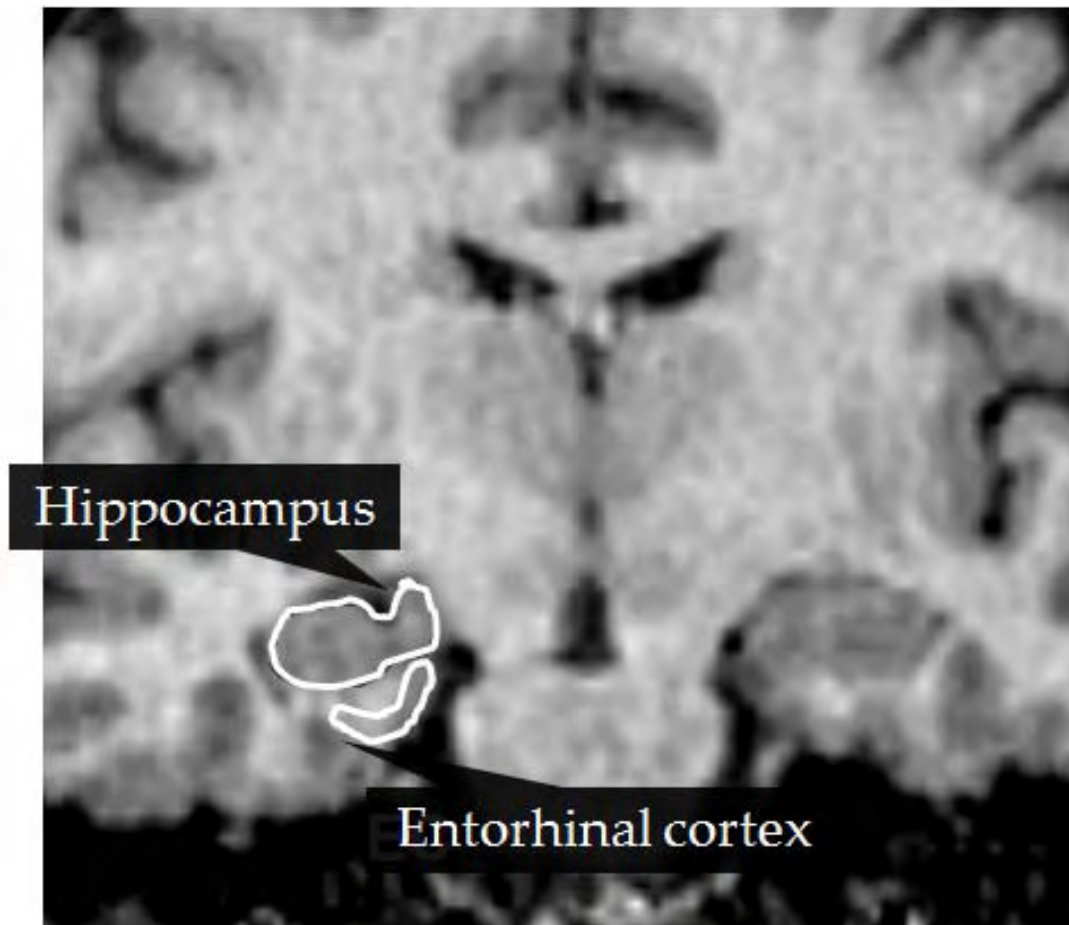
Fig. P4-1

3.3.6.3 3rd Ventricle

The anterior boundary was defined as where the lower portion of the ventricle opens into the CSF at the outer brain surface, and the posterior end was where the superior colliculi first fuse with the cerebrum. The crus of fornix and the prolonged line from it formed the superior border. The border of CSF served as the other boundaries.

3.3.6.4 Lateral Ventricle

All of the CSF areas of the lateral ventricle were included with the exception of the choroid plexus.

3.3.6.5 ICV

All structures inside the inner table of the skull were included: total brain, dura, ventricles and extraventricular CSF, brain stem and cerebellum. The boundary between spinal medulla and brain stem is considered to be at the level of the bottom of the cerebellum.

3.4 STATISTICAL METHODS

3.4.1 Statistical analysis for Paper 1

Discriminant Analysis is a multivariate statistical classification technique used to determine which variables that best discriminate between two or more groups, given several quantitative (independent) variables and a categorical (dependent) variable. The method extracts discriminant functions and models, which are linear combinations of the original quantitative variables selected. Discriminant Analysis was used to determine which CT linear measurements and which clinical variables best discriminated between AD subjects and the control subjects, as well as between AD+CVC and the controls. A forward stepwise discriminant procedure was used to select the independent variables that produced a good discrimination model. Colinearity tolerance of 0.4 was set to avoid the notable correlations between the independent variables. To eliminate the variables that provided superfluous information, the default F values of SPSS$^©$ (Statistical Package for the Social Sciences) were used (3.84 to enter and 2.71 to remove). Standardized canonical discriminant function coefficient, Matrix structure coefficient, Eigenvalues, Canonical correlation values and Wilks' Lambda were calculated.

ANOVA (Analysis of Variance) was used to compare each linear measurement between patients and controls, which was adjusted by age and gender.

3.4.2 Statistical analysis for Paper 2

Controlled by age and gender, partial correlation was used to separately examine the correlations between CSF biomarkers and CT measurements in the three groups of subjects (AD, AD+CVC, controls).

Discriminant analysis by STATISTICA$^©$ was performed to determine how CSF biomarkers or CT linear measurements contribute to the classifications of AD with or without CVC from controls. A forward stepwise discriminant procedure was used to select the independent variables that produced a successful discrimination model. Colinearity tolerance of 0.4 was set to avoid the notable correlations between the independent CT variables. To eliminate the variables that provided superfluous information, the F values were used as 3.84 to enter and 2.71 to remove. Standardized canonical discriminant function coefficient, Factor structure coefficient, and the percentages of correct classification for each group were achieved.

ANOVA was used to compare CSF biomarkers between the two groups of patients and the controls, which were controlled by age and gender.

3.4.3 Statistical analysis for Paper 3

Normal brain values (volume) in gender groups were described by descriptive statistics by STATISTICA$^©$. MANOVA (Multivariate Analysis of Variance) was used to compare the differences of brain structure volumes between women and men, adjusted

by age, ICV, and education. Dependent T-test was performed to identify the difference of hippocampus volume between the right and left side. Lateral asymmetry of hippocampus was defined as the absolute value of (Right - Left) / 0.5*(Right +Left). By multiple regression analysis, the contributions of age, gender and education to volumes were analyzed. To avoid the influence of ICV on volumes, the volumes used in multiple regression analyses were normalized by the mean of ICV. The rate of AAT, which is defined as the percentage volume change per year, was calculated from the regression coefficients (B value) in the regression equations, divided by the mean volume. The mean volumes of each age group were demonstrated to observe the possible age points of atrophy acceleration. To confirm this age point, piecewise regression analyses in different age ranges were performed.

3.4.4 Statistical analysis for Paper 4

The statistical difference between men and women in the characteristics of participants was tested with ANOVA for continuous variables and with chi-square test for categorical variables. The volumes of hippocampus and entorhinal cortex were corrected by dividing the individual volumes by total ICV and then multiplying the mean ICV volume, i.e., corrected volume = (raw volume / raw ICV)*mean raw ICV. A histogram showed that the distributions of the corrected hippocampal and entorhinal cortex volumes appeared to be normal. Multivariate general linear models were used to estimate the regression coefficient (β) and 95% confidence interval (CI) of hippocampus and entorhinal cortex volumes in relation to vascular risk factors and MMSE score. To evaluate the effect of multiple vascular factors on brain regional volumes, we developed the vascular risk factor score by counting the number of vascular risk factors that showed a tendency of negatively affecting either hippocampus or entorhinal cortex or both areas. The analyses were performed on the whole sample and stratified by gender controlling for demographic features, vascular risk factors and disorders, and the severity of white matter hyperintensities. Since controlling for white matter hyperintensity variables did not change the results, we only reported the results from two main models: model 1 was controlled for age, gender, and education, and in model 2 additional adjustment was made for all vascular factors and disorders measured (if the factors were not included in the vascular risk factor score) and MMSE score. All analyses were completed with the SPSS 15.0 for Windows.

4 RESULTS

4.1 PAPER 1

4.1.1 The two best linear measurements

In two discriminant analyses, a total of 20 variables (gender, age, ApoE genotype, systolic blood pressure, diastolic blood pressure, instable blood pressure (estimated with ortostatic blood pressure measurement), the 3 head size measurements, and the 11 combined indices and ratios of linear measurements) were selected as independent variables, and the diagnoses (controls vs. AD, controls vs. AD+CVC) as categorical variables (Table P1-2). With adjustment of age and gender, many of the linear measurements revealed significant differences between patients and controls by ANOVA (Table P1-2). The original CT linear measurements, which form the components of the combined indices and ratios, were not included as independent variables in the statistical analyses. The cognitive scores (MMSE, ADAS) were included as the main diagnostic criteria and may, subsequently, largely overlay the contribution of linear measurements in discriminant function due to the potential interference between brain atrophy and cognitive functions. For this reason, they were not included as independent variables in the study.

Table P1-2. Demographic and clinical characteristics, results of the CT linear measurements in aged normal controls, AD and AD+CVC patients

	Controls n=59		AD n=162		AD+CVC n=86	
	Mean	SD	Mean	SD	Mean	SD
Gender (male / female)	20 / 39		49 / 113		31 / 55	
Age (years old)	73	8	74	7	77	5
Systolic blood pressure (mmHg)	141	19	148	22	147	23
Diastolic blood pressure (mmHg)	80	8	83	12	82	12
Instable blood pressure (yes / no)	8 / 51		50 / 112		18 / 48	
MMSE	29	1	21	5	21	5
ADAS (85 points)	8	3	29	11	30	12
ADAS (70 points)	5	2	19	10	21	10
Apo-E4 (yes / no)	17 / 42		119 / 43		60 / 26	
Maximal transversal intracranial width (A)*	133.07	4.87	133.52	5.54	133.77	6.13
Maximal longitudinal intracranial width (B)*	168.88	6.31	167.8	6.89	167.59	7.76
Maximal width of frontal skull (C)*	118.16	4.43	118.35	5.72	118.07	6.31
Evans ratio (E/C)	0.315	0.035	0.331 [††]	0.038	0.332 [††]	0.040
Bicaudate ratio (F/A)	0.130	0.023	0.146 [†††]	0.030	0.148 [†††]	0.024
Huckman number (E+F)*	54.60	6.90	58.75 [†††]	8.04	58.94 [†††]	7.96
Cella media index (G/A)	0.205	0.041	0.219 [†]	0.041	0.222 [††]	0.039
3rd ventricular ratio (H/A)	0.054	0.015	0.066 [†††]	0.018	0.078 [††]	0.054
Ventricle index (J/E)	1.877	0.189	1.885	0.183	1.925	0.197
Frontal subarachnoid ratio (I/B)	0.015	0.008	0.018 [†]	0.007	0.017	0.010
Four cortical sulci ratio (M/A)	0.095	0.027	0.103	0.034	0.101	0.035
Cistern ambiens ratio (N/A)	0.025	0.007	0.026	0.008	0.028 [†]	0.008
Temporal horn ratio (O/A)	0.025	0.010	0.038 [†††]	0.017	0.044 [†††]	0.016
Suprasellar cistern ratio (P/A)	0.181	0.026	0.205 [†††]	0.029	0.211 [†††]	0.036

In CT linear measurements, brain size and the indices and ratios are shown in the table, original measurements that were not involved in the input of the discriminant function analysis are not shown here. ANOVA was used to compare each linear measurement between patients and controls, which was adjusted by age and gender. Significant results are marked.
[†] 0.01<=P<0.05; [††] 0.001<=P<0.01; [†††] P<0.001.
* The unit of the CT linear measurements is cm.

The forward stepwise discriminant analysis of controls vs. AD successfully produced an auto-fitting model (p<0.001) that included six variables with different standardized canonical discriminant function coefficients and matrix structure coefficients (Table P1-3).

Table P1-3. Standardized canonical discriminant function coefficients (1) and structure matrix (2), in controls *vs.* AD		
	1	2
Apo-E4	0.57	0.56
Temporal horn ratio (O/A)	-0.63	-0.51
Suprasellar cistern ratio (P/A)	-0.56	-0.52
Cistern ambiens ratio (N/A)	0.42	-0.05
Maximal longitudinal intracranial width (B)	0.31	0.12
Frontal subarachnoid ratio (I/B)	-0.25	-0.19

Model parameters in terms of percentage of explained variance: eigenvalues, canonical correlation values and Wilks' Lambda were reported (Table P1-4). Wilks' Lambda for controls vs. AD was 0.62, which implied a good discriminating power for the model.

Table P1-4. Discriminant Statistics: Summary of canonical discriminant functions						
	Eigenvalue	Canonical R	Wilks' Lambda	Chi Square	df	P-level
Controls *vs.* AD	0.62	0.62	0.62	91.10	7	<0.001*
Controls *vs.* AD+CVC	1.16	0.73	0.46	98.07	7	<0.001*
* P-level shows the models (discriminant functions) are significant (< 0.05).						

Besides Apo-E4 genotype, five CT linear measurements were achieved in the model. According to 0.3, the cut-off of coefficients [101], Apo-E4, suprasellar cistern ratio (P/A) and temporal horn ratio (O/A) were the three factors that contributed most significantly to the discrimination between AD and the controls. However, the other three variables in the model: maximal longitudinal intracranial width (B), cistern ambiens ratio (N/A) and frontal subarachnoid ratio (I/B), showed higher standardized canonical discriminant function coefficients (used to compare the relative importance of the independent variables; the higher their absolute value, the greater their unique contribution to the discriminant power), but lower matrix structure coefficients (global coefficients, not partial, that show the correlations of each variable in the model and reflect the uncontrolled association of the discriminating variables with the categorical variable) [101]. This means that the last three linear measurements may have partial effects on the discriminant function through overlay with the first four main variables, although they do contribute considerably to the discriminant function individually. Seven variables were included in the discriminant model for controls vs. AD+CVC (Table P1-5).

Table P1-5. Standardized canonical discriminant function coefficients (1) and Structure matrix (2), in controls *vs.* AD+CVC

	1	2
Temporal horn ratio (O/A)	-0.56	-0.67
Apo-E4	0.41	0.37
Suprasellar cistern ratio (P/A)	-0.42	-0.50
Instable blood pressure	-0.39	-0.23
Ventricle index (J/E)	-0.71	-0.11
Evans ratio (E/C)	-0.78	-0.21
Cella media index (G/A)	0.36	-0.20

Wilks' Lambda for controls vs. AD+CVC was 0.46 (p<0.001) showing the positive effect of the model (Table 4). The same three variables as for controls vs. AD (temporal horn ratio (O/A), suprasellar cistern ratio (P/A) and Apo-E4) were most significant. Instable blood pressure and the other three linear measurements with weaker contribution were also selected in the model.

4.1.2 Classification

The discriminant model for controls vs. AD correctly classified 90.2% of the AD cases and 68.3% of the controls. The corresponding values for controls vs. AD+CVC were 86.5% of AD+CVC cases and 88.3% of the controls (Table P1-6). The total percentages of correct classification for the two models were 84.3% and 87.3% respectively.

Table P1-6. Classification results of discriminant analysis.

	Controls *vs.* AD			Controls *vs.* AD+CVC		
	Controls	AD	Total	Controls	AD+CVC	Total
Percent correct (%)*	68.3	90.2	84.3	88.3	86.5	87.3
* The percentage of correct classification in groups.						

4.2 PAPER 2

4.2.1 Subjects characteristics

Subject characteristics in the three groups (controls, pure AD, and AD+CVC patients) are shown in Table P2-1. The original CT linear measurements, which form the components of the combined indices and ratios, were not included as independent variables in the statistical analyses. Considering the fact that the combined CT indices and ratios are 2D assessments of brain atrophy, brain size (maximal transversal intracranial width (A), maximal longitudinal intracranial width (B), and maximal width of frontal skull (C)) was included in some of the statistical analyses to avoid possible bias inducted by individual brain size. With adjustment for age and gender, the

ANOVA revealed significant differences between patients and controls in many of the linear measurements. The results were similar in the two groups of patients as compared with the controls. In particular, Evans ratio (E/C), bicaudate ratio (F/A), Huckman number (E+F), 3rd ventricular ratio (H/A), temporal horn ratio (O/A), and suprasellar cistern ratio (P/A) showed more significant differences ($p<0.01$) than the other CT measurements.

Table P2-1. Demographic and clinical characteristic results of the CT linear measurements and CSF biomarkers in aged normal controls, pure AD and AD+CVC patients

	Controls n=59		pure AD n=162		AD+CVC n=86	
	Mean	SD	Mean	SD	Mean	SD
Gender (male / female)	20 / 39		49 / 113		31 / 55	
Age (years old)	73	8	74	7	77	5
MMSE	29	1	21	5	21	5
Apo-E4 (yes / no)	17 / 42		119 / 43		60 / 26	
Total tau (T-tau)*	332.79	154.36	636.21[†††]	312.06	583.61[†††]	329.29
Phosphorylated tau (P-tau)*	61.52	17.41	79.97[†††]	30.01	70.17	32.98
Amyloid beta (1-42) (Abeta42)*	700.83	184.06	412.81[†††]	87.88	406.61[†††]	106.97
Maximal transversal intracranial width (A)**	133.07	4.87	133.52	5.54	133.77	6.13
Maximal longitudinal intracranial width (B)**	168.88	6.31	167.80	6.89	167.59	7.76
Maximal width of frontal skull (C)**	118.16	4.43	118.35	5.72	118.07	6.31
Evans ratio (E/C)	0.315	0.035	0.331[††]	0.038	0.332[††]	0.040
Bicaudate ratio (F/A)	0.130	0.023	0.146[†††]	0.030	0.148[†††]	0.024
Huckman number (E+F)**	54.60	6.90	58.75[†††]	8.04	58.94[†††]	7.96
Cella media index (G/A)	0.205	0.041	0.219[†]	0.041	0.222[††]	0.039
3rd ventricular ratio (H/A)	0.054	0.015	0.066[†††]	0.018	0.078[††]	0.054
Ventricle index (J/E)	1.877	0.189	1.885	0.183	1.925	0.197
Frontal subarachnoid ratio (I/B)	0.015	0.008	0.018[†]	0.007	0.017	0.010
Four cortical sulci ratio (M/A)	0.095	0.027	0.103	0.034	0.101	0.035
Cistern ambiens ratio (N/A)	0.025	0.007	0.026	0.008	0.028[†]	0.008
Temporal horn ratio (O/A)	0.025	0.010	0.038[†††]	0.017	0.044[†††]	0.016
Suprasellar cistern ratio (P/A)	0.181	0.026	0.205[†††]	0.029	0.211[†††]	0.036

In CT linear measurements, brain size and the indices and ratios are shown in the table. Original measurements that were not involved in the input of the discriminant function analysis are not shown here. ANOVA was used to compare each linear measurement between patients and controls, which was adjusted by age and gender. Significant results are marked.

† $0.01 <= P < 0.05$; †† $0.001 <= P < 0.01$; ††† $P < 0.001$

* The unit of the CSF biomarkers is pg/ml.

** The unit of the CT linear measurements is mm.

For CSF biomarkers, Aβ42 was decreased and T-tau was increased in both of the two patient groups compared to the controls. P-tau, however, was significantly increased only in the pure AD group, but not in the AD+CVC group. All ANOVA analyses performed were controlled by age and gender.

Table P2-2. Partial Correlations results between CSF biomarkers and CT linear measurements

	Controls			Pure AD			AD+CVC		
	T-tau	Abeta42	P-tau	T-tau	Abeta42	P-tau	T-tau	Abeta42	P-tau
Evans ratio (E/C)	0,05	0,11	-0,05	-0,23[††]	0,23[††]	-0,26[††]	-0,17	0,18	-0,26[†]
Bicaudate ratio (F/A)	-0,17	0,06	-0,21	-0,24[††]	0,05	-0,26[††]	-0,08	0,11	-0,19
Huckman number (E+F)	-0,08	0,07	-0,09	-0,25[††]	0,16	-0,30[†††]	-0,17	0,08	-0,19
Cella media index (G/A)	-0,76[†]	0,05	-0,31	-0,24[††]	0,13	-0,26[††]	-0,16	0,03	-0,20
3rd ventricular ratio (H/A)	-0,21	0,01	-0,24	-0,28[†††]	0,15	-0,29[†††]	-0,23	0,00	-0,23
Ventricle index (J/E)	-0,07	-0,16	0,07	0,20[†]	-0,18[†]	0,12	0,05	-0,13	0,13
Frontal subarachnoid ratio (I/B)	0,05	-0,16	0,13	-0,10	-0,11	-0,08	0,13	0,06	0,15
Four cortical sulci ratio (M/A)	0,10	-0,02	0,03	0,00	0,03	-0,03	0,13	-0,01	0,12
Cistern ambiens ratio (N/A)	-0,23	0,02	-0,19	-0,03	0,08	-0,15	0,01	0,18	-0,11
Temporal horn ratio (O/A)	-0,22	-0,02	-0,23	-0,15	0,12	-0,21[††]	0,02	0,09	0,02
Suprasellar cistern ratio (P/A)	-0,05	-0,11	0,01	-0,03	0,07	-0,09	-0,14	0,09	-0,14

Partial Correlations were controlled by age and gender. R value is presented in the table. Three measurements of brain size that had no correlations with CSF biomarkers are not showed in the table. Marked correlations are significant. †: 0.01<=P<0.05; ††: 0.001<=P<0.01; †††: P<0.001.

4.2.2 Correlation between CSF markers and CT measurements

Partial correlation adjusted by age and gender was used to separately examine the correlations between the three CSF biomarkers and the 14 CT measurements in the three groups. In the pure AD group, many CT measurements were found to significantly correlate with the three CSF biomarkers (r = 0.18-0.30) (Table P2-2),

besides temporal horn ratio (O/A) correlated with P-tau (r = 0.21). In contrast to the numerous correlations found in the pure AD group, there was only one significant correlation in each of the other two groups. T-tau correlated with the cella media index (G/A) in the control group(r = -0.76), and P-tau and Evans ratio (E/C) were correlated in the AD+CVC group (r = -0.26).

4.2.3 Results of discriminant analysis

To assess how CSF biomarkers and/or CT linear measurement contribute to the diagnosis of AD with or without CVC from controls, discriminant analysis was performed (Table P2-3). Firstly, the three CSF biomarkers, age and gender were selected as independent variables, and the diagnoses (controls vs. pure AD, controls vs. AD+CVC) as categorical variables. The forward stepwise discriminant analysis of controls vs. AD successfully produced an auto-fitting model (p<0.001) that included all of the 3 CSF variables with different standardized canonical discriminant function coefficients and matrix structure coefficients. However the model concerning controls vs. AD+CVC included only Aβ42. The discriminant model for controls vs. AD correctly classified 97.7% of the pure AD cases and 82.1% of the controls. The corresponding values for controls vs. AD+CVC were 94.4% of AD+CVC cases and 79.5% of the controls. Including the 14 CT measurements as additional independent variables into the second discriminant analysis, the 3 CSF biomarkers and temporal horn ratio (O/A) were introduced into the final model both in controls vs. pure AD and controls vs. AD+CVC. When discriminating pure AD from controls, the percentage of correct classification of pure AD was 98.1%, and 82.1% for controls. The corresponding values of correct classification AD+CVC were 96.5% and 84.6% for the controls. Obviously, there is a notable increase (from 79.5% to 84.6%) in the correct classification of controls from AD+CVC. However, there was hardly any added value in the classification of the controls from pure AD, when the CT measurements were combined with CSF biomarkers as independent variables.

Table P2-3-1. Discriminant Analyses between Pure AD and Controls

	Variables in the model	Standardized Coefficients	Factor Structure Coefficients	Correct Classification of Patients	Correct Classification of Controls
CSF biomarkers	Abeta42	-0,98	-0,91		
	T-tau	0,61	0,38	97,7%	82,1%
	P-tau	-0,52	0,24		
CSF biomarkers combined with CT linear measurements	Abeta42	-0,92	-0,86		
	Temporal horn ratio (O/A)	0,33	0,27	98,1%	82,1%
	T-tau	0,58	0,36		
	P-tau	-0,42	0,23		

Table P2-3-2. Discriminant Analyses between AD+CVC and Controls

	Variables in the model	Standardized Coefficients	Factor Structure Coefficients	Correct Classification of Patients	Correct Classification of Controls
CSF biomarkers	Abeta42	#	#	94,4%	79,5%
CSF biomarkers combined with CT linear measurements	Abeta42	0,93	0,71		
	Temporal horn ratio (O/A)	-0,42	-0,43	96,5%	84,6%
	P-tau	0,96	-0,10		
	T-tau	-0,87	-0,29		
# Since there is only one variable included successfully in the discriminant model, Canonical Analysis cannot be performed.					

CSF Aβ42 showed the largest contribution to both diagnoses of pure AD and of AD+CVC (Fig. P2-1), regardless of the presence of CT measurements. Combined with CSF biomarkers, temporal horn ratio (O/A), which most reflects MTA, was the only single measurement that was successfully involved in the final discriminant model for controls vs. AD or controls vs. AD+CVC.
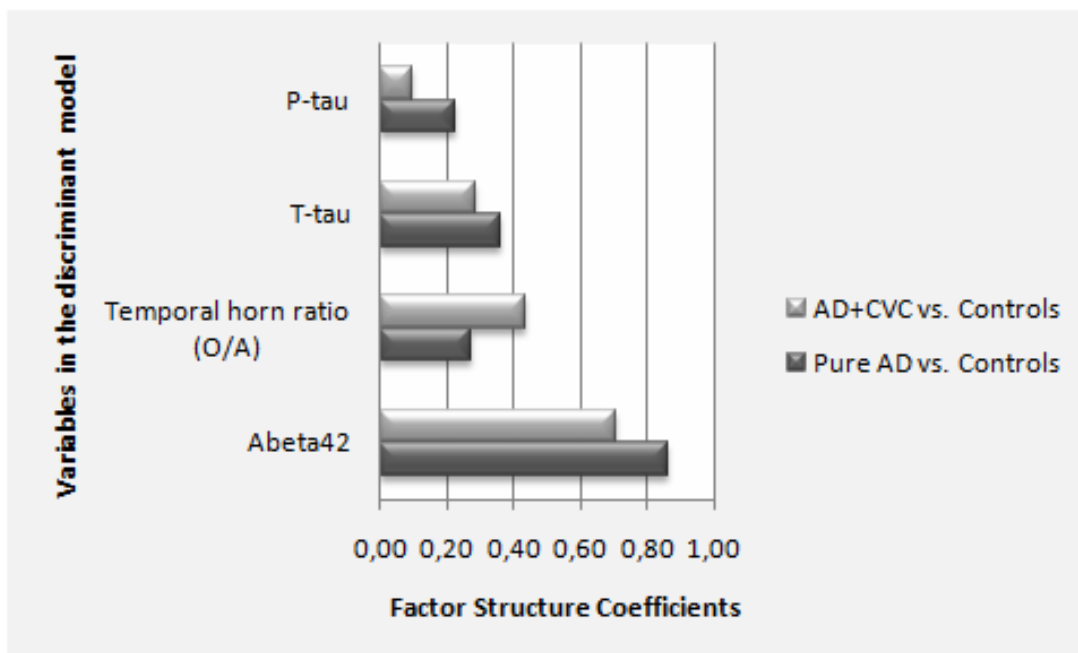
Fig. P2-1. Factor structure coefficients of the variables in the discriminant models by using CSF Biomarkers combined with CT linear measurements.

4.3 PAPER 3

4.3.1 Normal status of brain volume

4.3.1.1 *Descriptive statistics*

The raw values of the brain volumes together with demographic data are presented in Table P3-1. The range between maximum (2093.55 cm3) and minimum (1091.60 cm3) of ICV in the study was rather large, which reflects the substantial variation in head size of the subjects. A large variation of the volumes of the lateral ventricles was accordingly seen in that the ratio between its maximum and minimum volume was 48 (123.40 cm3/ 2.60 cm3). The mean ± 1.96 * the standard deviation of total hippocampus volume in males was 6.99 ± 1.84 cm3, and in females 6.49 ± 1.65 cm3. The raw brain volumes for each age group are shown in Table P3-2.

Table P3-1: Descriptive statistical, MONOVA and Dependent T-test results of demographic data and brain structures volumes

	Female (n = 318)				Male (n = 226)			
	Mean	Mini.	Maxi.	S.D.	Mean	Mini.	Maxi.	S.D.
Age (years old)	71,7	60	97	8,9	70,7	60	94	9,1
Education (years) ***	11,9	5,00	23,00	3,8	13,5	3,00	23,00	4,3
ICV (cm3) ***	1402,7	1091,6	1743,4	105,3	1611,9	1313,1	2093,6	130,3
Lateral ventricle (cm3) ***	25,98	2,60	105,80	16,73	32,81	5,50	123,40	19,68
3rd ventricle (cm3) ***	1,42	0,30	3,20	0,61	1,84	0,50	5,30	0,69
Left hippocampus (cm3) ***	<u>3,21</u>	1,74	4,46	0,44	<u>3,46</u>	2,22	4,73	0,50
Right hippocampus (cm3) ***	<u>3,29</u>	1,89	4,66	0,43	<u>3,53</u>	2,13	5,13	0,48
Total hippocampus (cm3) ***	6,49	3,63	8,97	0,84	6,99	4,42	9,61	0,94
Lateral Symmetry of hippocampus	6,3%	0,0%	29,5%	4,8%	6,5%	0,0%	28,4%	5,1%

In the MANOVA results, the variables marked with *** present strong significant differences (P < 0.001) between the two gender groups.

The analysis of ICV was adjusted by age and education. The other analyses of brain structures were adjusted by age, ICV and education.

Also a strong significant difference (P < 0.001) was shown between left and right hippocampus volume by a Dependent T-test analysis.

 Lateral symmetry of hippocampus was defined as the absolute value of (Right - Left) / 0.5 * (Right +Left).

Table P3-2a: Intra cranial volume (ICV) by age groups

Age groups	No. of patients	Mean	Std.Dev.	No. of patients	Mean	Std.Dev.
	Female			Male		
60	76	1424,54	100,72	67	1678,65	139,95
66	72	1407,26	111,48	53	1606,08	122,46
72	55	1396,50	109,41	31	1555,97	130,73
78	46	1406,15	80,61	31	1581,32	112,81
81	32	1371,93	127,41	19	1571,20	84,66
84	18	1380,65	80,51	9	1562,70	96,96
90+	19	1380,69	113,61	16	1595,74	105,08

Table P3-2b: Raw volume of lateral ventricle (LV) by age groups

Age groups	No. of patients	Mean	Std.Dev.	No. of patients	Mean	Std.Dev.
	Female			Male		
60	76	18,90	15,59	67	24,69	15,31
66	72	21,71	13,26	53	28,06	15,94
72	55	24,69	11,92	31	31,57	18,96
78	46	32,73	20,96	31	43,24	25,96
81	32	32,28	14,52	19	46,85	15,41
84	18	34,27	15,10	9	40,32	16,48
90+	19	39,39	19,51	16	43,89	19,60

Table P3-2c: Raw volume of 3rd ventricle (3rd V) by age groups

Age groups	No. of patients	Mean	Std.Dev.	No. of patients	Mean	Std.Dev.
	Female			Male		
60	76	1,07	0,62	67	1,54	0,62
66	72	1,29	0,49	53	1,80	0,55
72	55	1,39	0,52	31	1,71	0,63
78	46	1,68	0,56	31	2,09	0,69
81	32	1,67	0,54	19	2,48	0,85
84	18	1,99	0,57	9	2,38	0,58
90+	19	1,80	0,57	16	1,89	0,52

Table P3-2d: Raw volume of Left hippocampus by age groups

Age groups	No. of patients	Mean	Std.Dev.	No. of patients	Mean	Std.Dev.
	Female			Male		
60	76	3,51	0,35	67	3,81	0,42
66	72	3,41	0,32	53	3,58	0,40
72	55	3,20	0,34	31	3,46	0,32
78	46	3,01	0,33	31	3,24	0,38
81	32	2,84	0,38	19	2,96	0,31
84	18	2,85	0,32	9	3,12	0,41
90+	19	2,62	0,39	16	2,79	0,36

Table P3-2e: Raw volume of Right hippocampus by age groups						
Age groups	No. of patients	Mean	Std.Dev.	No. of patients	Mean	Std.Dev.
	Female			Male		
60	76	3,56	0,39	67	3,81	0,42
66	72	3,45	0,31	53	3,65	0,44
72	55	3,27	0,33	31	3,51	0,43
78	46	3,20	0,33	31	3,38	0,29
81	32	2,88	0,35	19	3,15	0,32
84	18	3,02	0,38	9	3,19	0,37
90+	19	2,78	0,35	16	2,89	0,38
The unit of the volume is cm3.						

4.3.1.2 Gender differences

The gender differences were calculated using MANOVA (Table P3-1). The two gender groups did not differ by age. The male sample had received more education than the female sample. ICV was significantly larger (around 15%) in males than in females. The analysis of ICV was adjusted by age and education.

The MANOVA also revealed strongly significant ($p < 0.001$) gender differences in volume for all brain structures, after the adjustment for age, ICV and education. The lateral ventricles and 3rd ventricle were larger in males than that in females. The normalized volumes of left, right and total hippocampus in males were smaller than those in females, even if the mean of raw volumes were larger in males as shown in Table 1.

4.3.1.3 Lateral asymmetry

A strong significant difference ($p < 0.001$) was also observed between left and right hippocampus volume by a dependent T-test analysis. Right hippocampus was larger than the left, regardless of gender. The mean of the lateral asymmetry was around 6% between the left and right hippocampus. The maximum lateral difference was around 29%. Approximately 18% of the subjects had lateral differences over 10%. There was no significant gender difference of lateral asymmetry of hippocampus.

4.3.2 Rate of AAT

In the initial multiple regression analyses, age and gender but not education significantly ($p < 0.001$) contributed to all normalized brain volumes. An interaction of age*gender was also found to significantly ($p < 0.001$) contribute to the volumes. As education had no effect on the volumes, additional regression analyses (only age contributes to volume) were performed separately in the two gender groups for each of the brain structures. The rates of AAT (Aging Atrophy Trend - % decline per year) were calculated from the regression coefficient (B value) in the successful regression equations ($p < 0.001$), divided by mean volumes. (Fig. P3-2a) Total hippocampus volumes were reduced by 0.68% per year in males, and by 0.79% in females across the entire age span (60-87+ years). The rate of AAT for the expansion of the lateral ventricles (2.80%/year in males, 2.95%/year in females) and 3rd ventricle (1.58%/year in males, 2.28%/year in females) was larger than the estimated hippocampal shrinkage.

The rates of AAT were shown to be significantly faster in females than that in males due to the successfully interacted (age*gender) contribution to volumes. Due to the large volume changes in the two oldest age groups (Fig. P3-3), the analyses were repeated in subjects younger than 83 years. Similar results were obtained as for the full age range. (Fig. P3-2b)


**The speeds of AAT in male and female population**

	Lateral ventricle	3rd ventricle	Left hippocampus	Right hippocampus	Total hippocampus
Male	2,80%	1,58%	-0,76%	-0,60%	-0,68%
Female	2,95%	2,28%	-0,87%	-0,71%	-0,79%

Fig. P3-2a

The speeds of AAT in population aged less than 82y

|	Lateral ventricle	3rd ventricle	Left hippocampus	Right hippocampus	Total hippocampus
Male	3,71%	2,29%	-0,67%	-0,44%	-0,55%
Female	3,12%	2,45%	-0,83%	-0,70%	-0,77%

Fig. P3-2b

34
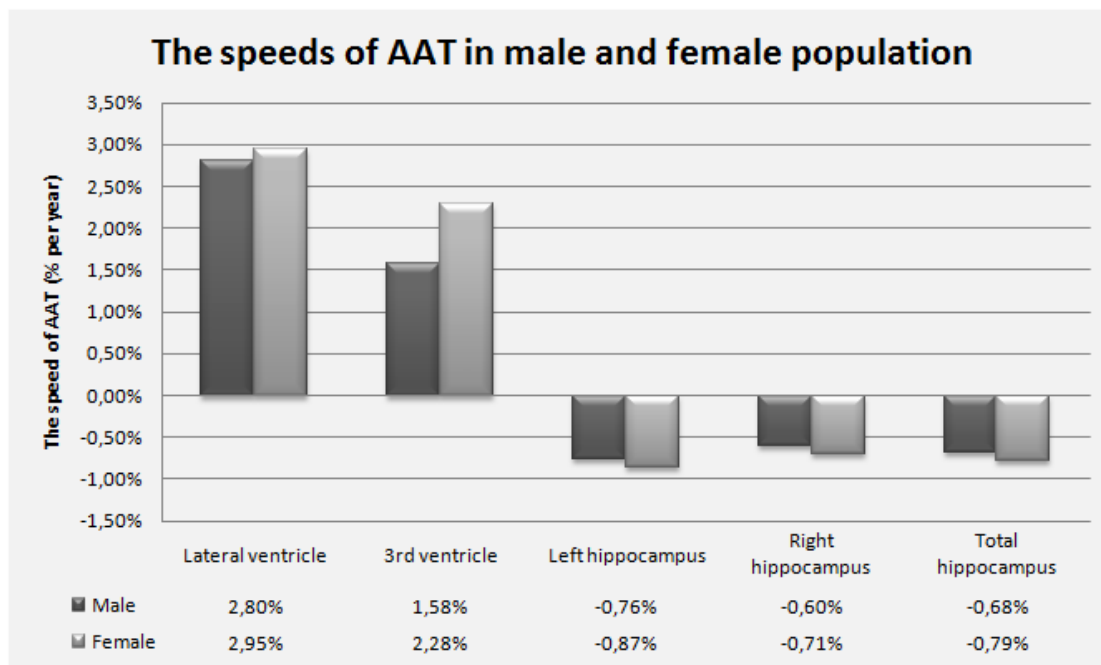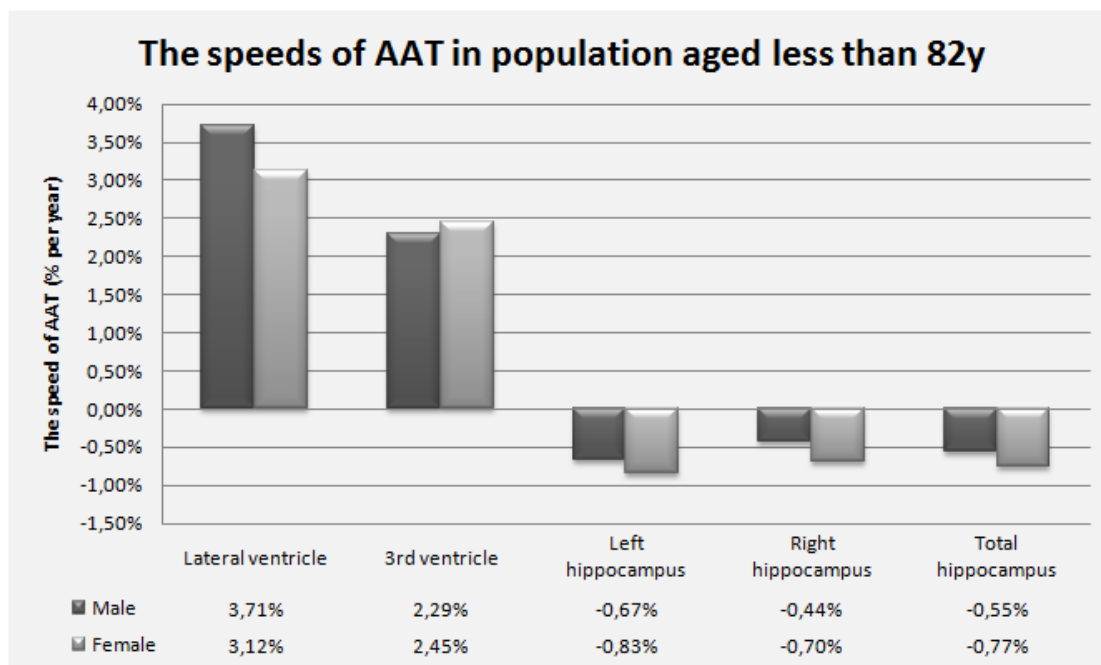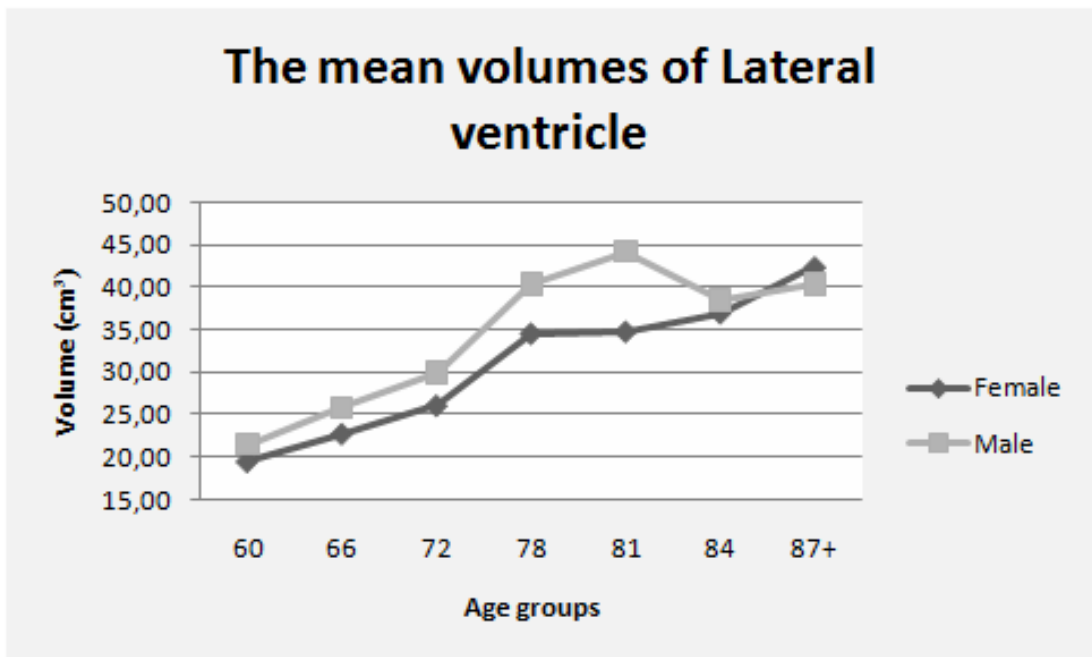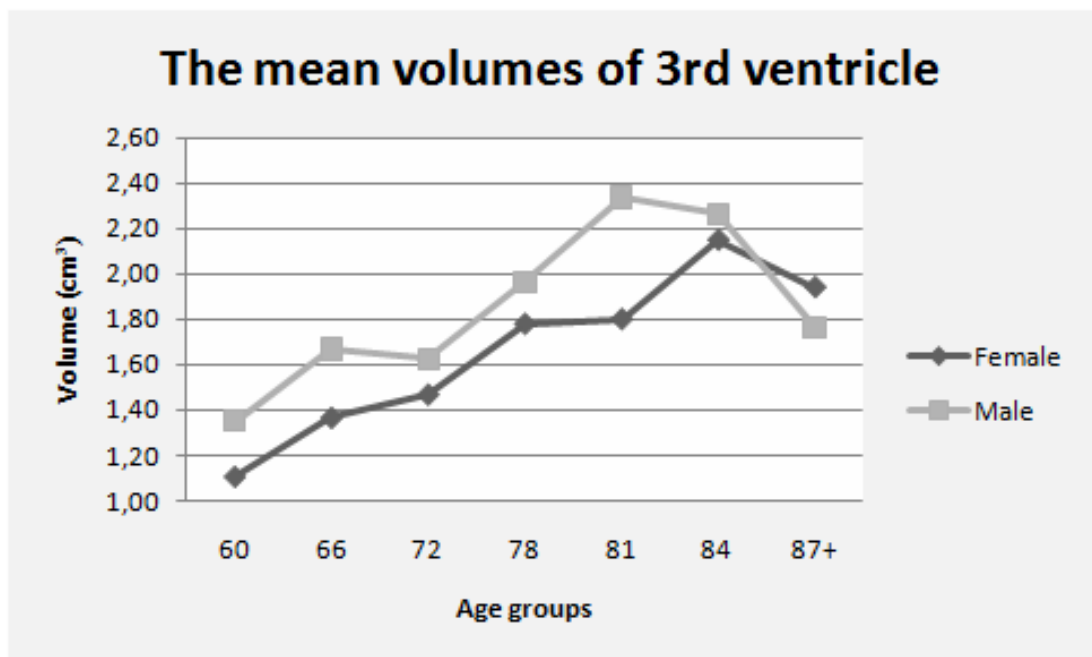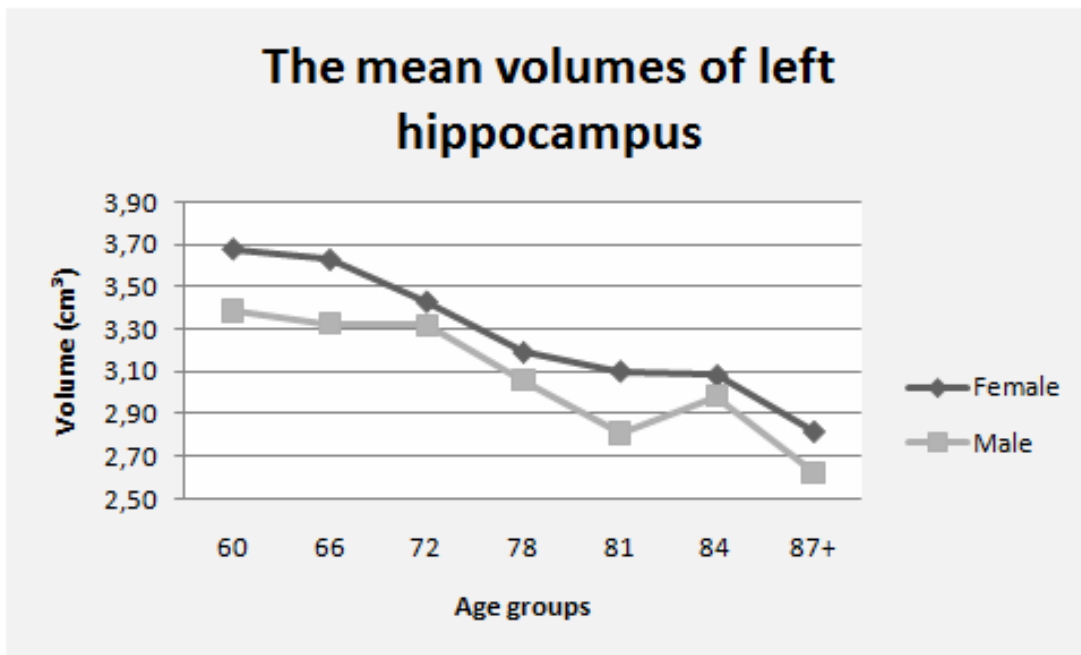
Fig. P3-3a

Fig. P3-3b

Fig. P3-3c
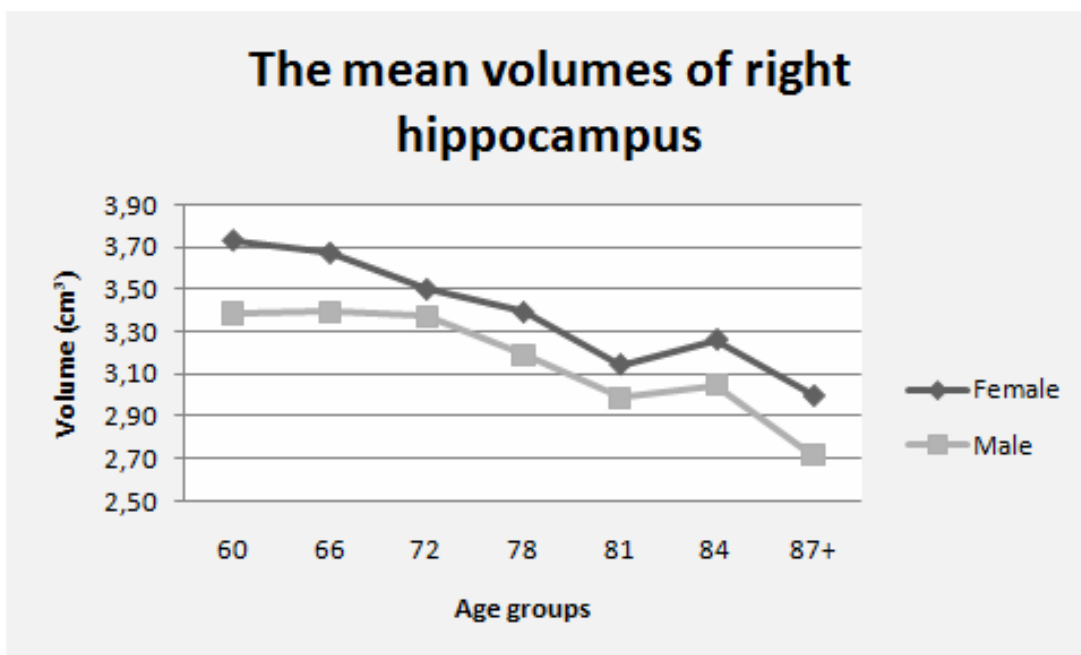
Fig. P3-3d
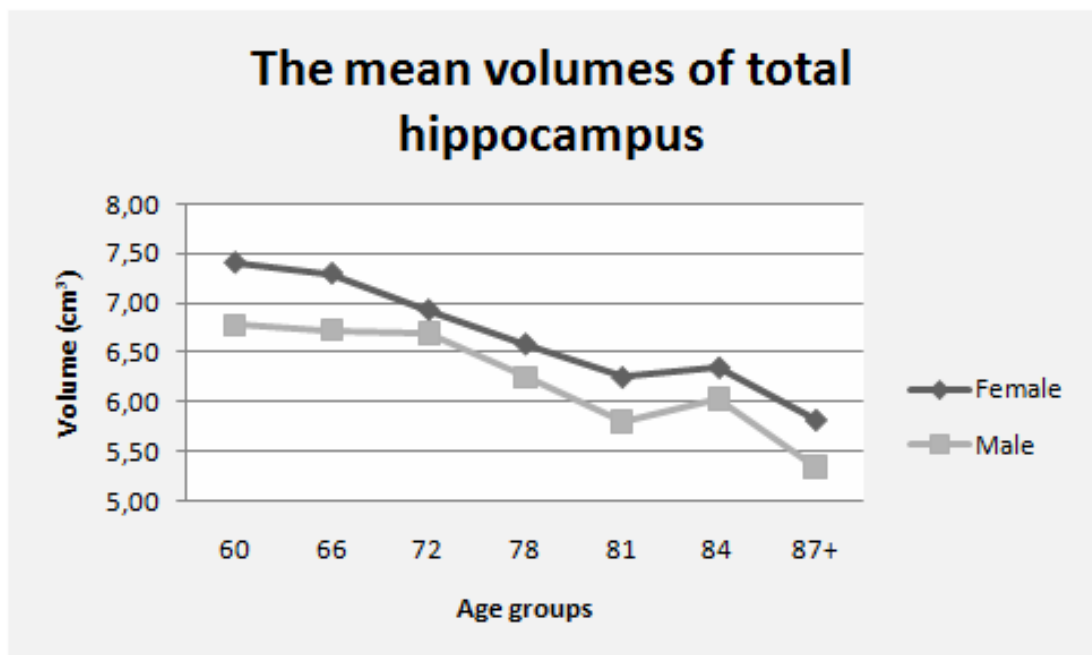
Fig. P3-3e

4.3.3 Acceleration of AAT

The mean normalized volumes in each age group were demonstrated in Fig. P3 in order to observe the possible age point at which atrophy acceleration starts. The significances of the possible turning age points from these observations were tested by Piecewise regression analyses. Only 72 years of age in total hippocampus volume in the whole gender group was the significant turning point. This shows that there was a significant difference in the atrophy slopes for total hippocampus before and after 72 years of age. This age point (72y) is suggested to represent the time when the acceleration of AAT in hippocampus starts in normal aging. The same attempts for other brain structures were negative.

4.4 PAPER 4

4.4.1 Characteristics

Table P4-1 shows the characteristics of the study participants by gender. Compared with women, men were more likely to have a higher level of education, to be a former smoker, to have a binge pattern of alcohol consumption, to have a history of diabetes and coronary heart disease, and to have a larger ICV volume. In addition, women tended to have a higher total cholesterol level.

Table P4-1. Characteristics of the study participants by gender

Characteristics	All (n=523)	Men (n=212)	Women (n=311)	p-value[*]
Age (years), mean (SD)	70.6 (9.1)	70.0 (9.1)	71.1 (9.0)	0.184
Education (years), mean (SD)	12.6 (4.1)	13.5 (4.3)	12.0 (3.8)	<0.001
Smoking, n (%)				
Never	232 (44.4)	78 (36.8)	154 (49.5)	
Former	217 (41.5)	105 (49.5)	112 (36.0)	
Current	74 (14.1)	29 (13.7)	45 (14.5)	0.006
Alcohol consumption, n (%)				
No or less than once a month	136 (26.0)	41 (19.3)	95 (30.5)	
Non-binge	342 (65.4)	137 (64.6)	205 (65.9)	
Binge	45 (8.6)	34 (16.0)	11 (3.5)	<0.001
Intensive physical activity, n (%)				
No	160 (30.6)	58 (27.4)	102 (32.8)	
Less than weekly	162 (31.0)	72 (34.0)	90 (38.9)	
Daily-to-weekly	138 (26.4)	59 (27.8)	79 (25.4)	
Not report/missing	63 (12.0)	23 (10.8)	40 (12.9)	0.398
BMI (kg/m^2), mean (SD)	25.9 (3.7)	26.0 (3.1)	25.9 (4.1)	0.723
Total cholesterol ≥6.5 mmol/L	167 (31.9)	59 (27.8)	108 (34.7)	0.095
Hypertension, n (%)	399 (76.3)	165 (77.8)	234 (75.2)	0.493
Diabetes mellitus, n (%)	34 (6.5)	19 (9.0)	15 (4.8)	0.062
Coronary heart disease, n (%)	62 (11.9)	36 (17.0)	26 (8.4)	0.003
MMSE score, mean (SD)	29.1 (1.1)	29.1 (1.1)	29.1 (1.1)	0.926
Total ICV (ml), mean (SD)	1488 (154)	1611 (130)	1404 (106)	<0.001
Hippocampal volume (ml, corrected), mean (SD)	6.73 (0.83)	6.47 (0.76)	6.91 (0.83)	<0.001
Entorhinal cortex volume (ml, corrected), mean (SD)	2.47 (0.36)	2.38 (0.31)	2.54 (0.37)	<0.001

ICV = intracranial volume; SD = standard deviation. [*]P-value was for the statistical comparison between men and women.

4.4.2 Brain volume and vascular risk factors

Among the whole sample, binge drinking was significantly associated with reduced volume of hippocampus, and diabetes was statistically related to a smaller volume of entorhinal cortex (Table P4-2). Furthermore, compared to never smokers, current smokers tended to have reduced volumes of hippocampus and entorhinal cortex, whereas former smokers had a larger volume of both regions. Finally, a higher MMSE score was significantly associated with larger volumes of hippocampus and entorhinal cortex.

Table P4-2. Beta coefficient (95% confidence interval, CI) of hippocampal and entorhinal cortex volumes related to vascular factors an MMSE score from multivariate general linear regression models

Characteristics	Hippocampus		Entorhinal cortex	
	Beta (95% CI)[†]	Beta (95% CI)[‡]	Beta (95% CI)[†]	Beta (95% CI)[‡]
Total (n=523)				
Smoking				
Former vs. never	0.096 (-0.032, 0.223)	0.127 (-0.003, 0.257)	0.076 (0.011, 0.140)	0.080 (0.014, 0.146)
Current vs. never	-0.138 (-0.319, 0.043)	-0.111 (-0.294, 0.072)	-0.023 (-0.115, 0.069)	-0.029 (-0.122, 0.065)
Alcohol consumption				
Non-binge vs. no	-0.080 (-0.218, 0.058)	-0.102 (-0.242, 0.038)	0.036 (-0.034, 0.107)	0.025 (-0.046, 0.097)
Binge vs. no	-0.295 (-0.536, -0.055)	-0.315 (-0.559, -0.072)	-0.011 (-0.134, 0.112)	-0.033 (-0.158, 0.091)
Physical activity				
Less than weekly vs. no	-0.040 (-0.191, 0.111)	-0.030 (-0.181, 0.120)	-0.020 (-0.098, 0.057)	-0.023 (-0.100, 0.054)
Daily-to-weekly vs. no	0.080 (-0.078, 0.237)	0.077 (-0.080, 0.235)	0.017 (-0.063, 0.098)	0.010 (-0.070, 0.091)
Missing vs. no	0.038 (-0.160, 0.237)	0.053 (-0.147, 0.252)	-0.024 (-0.125, 0.077)	-0.015 (-0.117, 0.087)
BMI (kg/m^2)	0.007 (-0.009, 0.023)	0.005 (-0.011, 0.021)	0.000 (-0.008, 0.008)	-0.001 (-0.009, 0.007)
High cholesterol (≥6.5 mmol/L)	-0.084 (-0.209, 0.041)	-0.059 (-0.187, 0.069)	-0.032 (-0.096, 0.031)	-0.029 (-0.095, 0.036)
Hypertension	-0.021 (-0.161, 0.119)	-0.013 (-0.156, 0.130)	-0.011 (-0.083, 0.060)	-0.006 (-0.079, 0.067)
Diabetes	-0.015 (-0.252, 0.222)	-0.067 (-0.307, 0.174)	-0.115 (-0.235, 0.005)	-0.136 (-0.259, -0.013)
Coronary heart disease	0.036 (-0.151, 0.223)	0.032 (-0.159, 0.223)	0.000 (-0.095, 0.096)	0.012 (-0.086, 0.109)
MMSE score	0.068 (0.012, 0.124)	0.075 (0.018, 0.131)	0.033 (0.005, 0.062)	0.034 (0.005, 0.063)

To be continued,

Table P4-2, continued,				
Men (n=212)				
Smoking				
Former vs. never	0.001 (-0.194, 0.197)	0.026 (-0.173, 0.225)	-0.001 (-0.094, 0.092)	-0.006 (-0.102, 0.091)
Current vs. never	-0.253 (-0.542, 0.036)	-0.278 (-0.570, 0.013)	-0.081 (-0.219, 0.057)	-0.081 (-0.223, 0.060)
Alcohol consumption				
Non-binge vs. no	-0.197 (-0.432, 0.037)	-0.153 (-0.388, 0.082)	-0.012 (-0.124, 0.100)	0.007 (-0.108, 0.121)
Binge vs. no	-0.324 (-0.633, -0.014)	-0.311 (-0.624, 0.002)	-0.035 (-0.183, 0.114)	-0.045 (-0.197, 0.107)
Physical activity				
Less than weekly vs. no	-0.094 (-0.330, 0.143)	-0.112 (-0.348, 0.123)	0.037 (-0.076, 0.150)	0.028 (-0.087, 0.142)
Daily-to-weekly vs . no	0.047 (-0.196, 0.290)	0.076 (-0.169, 0.321)	0.034 (-0.082, 0.150)	0.038 (-0.081, 0.156)
Missing vs. no	0.181 (-0.142, 0.504)	0.171 (-0.153, 0.495)	0.013 (-0.141, 0,167)	-0.012 (-0.169, 0.146)
BMI (kg/m^2)	0.010 (-0.019, 0.039)	-0.001 (-0.031, 0.029)	0.009 (-0.005, 0.023)	0.009 (-0.006, 0.023)
High cholesterol ($\geq$6.5 mmol/L)	-0.255 (-0.452, -0.058)	-0.273 (-0.481, -0.066)	-0.105 (-0.199, -0.012)	-0.118 (-0.218, -0.017)
Hypertension	-0.027 (-0.247, 0.193)	0.025 (-0.199, 0.249)	0.014 (-0.091, 0.119)	0.022 (-0.086, 0.131)
Diabetes	0.041 (-0.275, 0.356)	0.042 (-0.280, 0.364)	-0.114 (-0.263, 0.035)	-0.143 (-0.300, 0.013)
Coronary heart disease	-0.020 (-0.266, 0.225)	-0.050 (-0.300, 0.200)	-0.008 (-0.125, 0.109)	-0.010 (-0.132, 0.111)
MMSE score	0.076 (-0.009, 0.161)	0.070 (-0.015, 0.155)	0.015 (-0.025, 0.056)	0.010 (-0.031, 0.051)

To be continued,

Table P4-2, continued,

Women (n=311)

Smoking				
Former vs. never	0.144 (-0.027, 0.314)	0.167 (-0.010, 0.345)	0.119 (0.028, 0.209)	0.124 (0.031, 0.218)
Current vs. never	-0.066 (-0.297, 0.165)	-0.052 (-0.293, 0.189)	0.006 (-0.117, 0.129)	-0.017 (-0.144, 0.111)
Alcohol consumption				
Non-binge vs. no	-0.034 (-0.205, 0.137)	-0.073 (-0.250, 0.105)	0.054 (-0.037, 0.146)	0.030 (-0.064, 0.123)
Binge vs. no	-0.322 (-0.754, 0.110)	-0.350 (-0.802, 0.102)	0.005 (-0.226, 0.235)	0.001 (-0.238, 0.239)
Physical activity				
Less than weekly vs. no	0.020 (-0.177, 0.217)	0.040 (-0.159, 0.240)	-0.054 (-0.159, 0.051)	-0.060 (-0.165, 0.046)
Daily-to-weekly vs. no	0.113 (-0.097, 0.322)	0.103 (-0.108, .0315)	0.000 (-0.112, 0.112)	-0.001 (-0.113, 0.110)
Missing vs. no	-0.043 (-0.293, 0.208)	-0.002 (-0.261, 0.257)	-0.049 (-0.183, 0.084)	-0.026 (-0.163, 0.110)
BMI (kg/m2)	0.005 (-0.014, 0.024)	0.003 (-0.017, 0.022)	-0.004 (-0.014, 0.006)	-0.006 (-0.016, 0.004)
High cholesterol (≥6.5 mmol/L)	0.009 (-0.152, 0.169)	0.041 (-0.127, 0.209)	0.012 (-0.074, 0.098)	0.027 (-0.062, 0.115)
Hypertension	0.000 (-0.181, 0.182)	0.011 (-0.180, 0.201)	-0.024 (-0.121, 0.073)	-0.023 (-0.124, 0.077)
Diabetes	-0.100 (-0.455, 0.255)	-0.159 (-0.529, 0.212)	-0.132 (-0.321, 0.057)	-0.145 (-0.340, 0.051)
Coronary heart disease	0.111 (-0.173, 0.395)	0.129 (-0.170, 0.429)	0.007 (-0.145, 0.159)	0.019 (-0.139, 0.177)
MMSE score	0.058 (-0.017, 0.133)	0.069 (-0.008, 0.147)	0.046 (0.006, 0.085)	0.053 (0.012, 0.093)

[*] Beta (95% CI) was derived from models controlling for age, gender, and education.
[†] Beta (95% CI) was derived from models including age, gender, education, and all variables in the table.

However, the associations between vascular factors and brain regional volumes appeared to vary by gender (Table P4-2). Among men, current smoking and binge alcohol consumption were significantly or marginally associated with the reduced volume of hippocampus, diabetes was marginally related to a smaller volume of entorhinal cortex, and high total cholesterol was significantly associated with the reduced volumes of both regions. MMSE score was marginally associated with larger volume of hippocampus, but not of entorhinal cortex. By contrast, of the vascular factors among women, only diabetes tended to be related to the reduced volume of entorhinal cortex, none of current smoking, binge drinking, high total cholesterol, and diabetes was significantly associated with the volume of hippocampus. Furthermore, the larger volumes of hippocampus and entorhinal cortex associated with former smoking were statistically or marginally evident only among women. Finally, among women an increasing MMSE score was statistically or marginally associated with larger volumes of the hippocampus and entorhinal cortex.

Intensive physical activity, BMI, hypertension, and a history of coronary heart disease were not associated with brain regional volumes in the whole sample or in either gender stratum.

4.4.3 Brain volume and scored multiple vascular risk factors

We further examined the burden of multiple vascular factors in association with the brain regional volumes, in which the vascular burden was scored by counting the number of vascular factors that showed negative effect on brain regional volumes, i.e., current smoking, binge drinking, high total cholesterol, and diabetes. In the whole sample, increasing burden of vascular risk factors was significantly associated with decreasing volumes of the hippocampus and entorhinal cortex in a dose-response manner (Table P4-3). Further analysis stratifying by gender suggested that such a dose-response relationship was statistically evident only among men. Among women, having two or more vascular factors was also associated with reduced volumes of hippocampus and entorhinal cortex, although the association was not statistically significant.

Table P4-3. Beta coefficient (95% confidence interval, CI) of hippocampal and entorhinal cortex volumes related to the burden of vascular risk factors from multivariate linear regression models

Vascular risk score[*], by gender	Hippocampus		Entorhinal cortex	
	Beta (95% CI)[†]	Beta (95% CI)[‡]	Beta (95% CI)[†]	Beta (95% CI)[‡]
Total (n=523)				
0 (n=257)	0 (Reference)	0 (Reference)	0 (Reference)	0 (Reference)
1 (n=217)	-0.102 (-0.225, 0.021)	-0.097 (-0.222, 0.028)	-0.025 (-0.087, 0.038)	-0.024 (-0.087, 0.040)
≥2 (n=49)	-0.287 (-0.496, -0.078)	-0.264 (-0.475, -0.053)	-0.146 (-0.253, -0.040)	-0.140 (-0.248, -0.032)
P for trend	0.006	0.011	0.020	0.029
Men (n=212)				
0 (n=95)	0 (Reference)	0 (Reference)	0 (Reference)	0 (Reference)
1 (n=94)	-0.192 (-0.381, -0.002)	-0.176 (-0.370, 0.018)	-0.050 (-0.139, 0.040)	-0.051 (-0.143, 0.042)
≥2 (n=23)	-0.482 (-0.783, -0.181)	-0.465 (-0.773, -0.157)	-0.264 (-0.406, -0.120)	-0.259 (-0.406, -0.112)
P for trend	0.001	0.003	0.002	0.002
Women (n=311)				
0 (n=162)	0 (Reference)	0 (Reference)	0 (Reference)	0 (Reference)
1 (n=123)	-0.032 (-0.192, 0.129)	-0.031 (-0.196, 0.135)	-0.007 (-0.093, 0.079)	0.005 (-0.083, 0.093)
≥2 (n=26)	-0.136 (-0.423, 0.151)	-0.127 (-0.420, 0.166)	-0.049 (-0.202, 0.104)	-0.041 (-0.196, 0.115)
P for trend	0.387	0.425	0.603	0.767

[*] The score = the number of factors including current smoking, binge alcohol consumption, diabetes, and high total cholesterol.

[†] Controlling for age, gender, and education.

[‡] Controlling for age, gender, education, BMI, physical activity, hypertension, coronary heart disease, and MMSE score.

5 DISCUSSION AND CONCLUSIONS

5.1 PAPER 1

5.1.1 Temporal horn ratio and suprasellar cistern ratio

Early diagnosis of AD is important considering effective upcoming treatment. It is difficult to differentiate AD from healthy controls in early stages while it is easier in the later stages using simple clinical assessments. In the study we used simple CT linear measurements to discriminate early AD from healthy aged controls.

Our main finding is that two CT linear measurements (temporal horn ratio and suprasellar cistern ratio) in combination with one clinical examination (genotype Apo-E4) can discriminate between AD patients and healthy aged controls as well as between AD+CVC and the controls.

The increases of temporal horn ratio (O/A) and suprasellar cistern ratio (P/A), which are the two most significant CT linear measurements in AD patients regardless of with or without CVC, reflect the independent enlargement of the temporal horns of lateral ventricle and that of supersellar cistern. Since they are adjacent to the medial temporal lobe [52, 102], the enlargements indicate medial temporal lobe atrophy in AD patients. Consequently, our study came to the same conclusions as previous MRI studies [11-13] in which MTA was found to be significant in AD patients. Since only AD patients showing mild and moderate disease were involved in our study, this is also consistent with previous findings of MTA being an early sign of AD [10]. In comparison with manual outlining of medial temporal lobe in MRI, the linear measurements are simple and rapid, and no extra software or 3D high-resolution images are required. Furthermore, considering the inexpensiveness and wide availability of CT, it would be much easier for clinicians and radiologists to adopt. Therefore, the two CT linear measurements can probably be of value in evaluating MTA in the work-up of AD instead of manual outlining in MRI.

The enlargements of temporal horn and suprasellar cistern correlated very little with each other in AD since both of them contributed together to one discriminant function. This may reflect that they represent partially different kinds of atrophy in the different anatomical parts. Considering the neighboring structures, enlargement of the temporal horn may for AD patients reflect atrophy in more parts of the temporal lobe than the medial temporal lobe. And the enlargement of the whole subarachnoid cisterns can in part yield the enlargement of the suprasellar cistern. To clarify the inference, further studies are needed.

5.1.2 Other linear measurements

Several other linear measurements also contributed to a lesser extent to the discrimination between AD patients and controls. Frontal subarachnoid ratio (I/B) may partially reflect frontal lobe atrophy, but the measurement had low reliability. Four cortical sulci ratio (M/A), that is the only direct measurement for assessment of cortical atrophy, were not involved into the final model at all. Whilst the end stages of AD are accompanied by a macroscopically detectable cortical atrophy [9], there are little indications, in this study at least, that cortical atrophy is helpful in the diagnoses of mild and moderate AD. Ventricle index (J/E), cella media index (G/A) and Evans ratio (E/C), which are more related to central atrophy, presented only weak contribution in

the discrimination between AD+CVC patients and the controls. This could result from the cerebrovascular abnormalities accompanying AD and therefore be related to central atrophy.

5.1.3 Apo-E4

It was again confirmed that Apo-E4 genotype is a strong marker for AD. Apo-E4, however, had little interaction with MTA in AD patients because they presented strong discriminating power together. This shows that the presence of the Apo-E4 genotype did not influence MTA in AD.

5.1.4 Conclusions of Paper1

In conclusion, we show that simple CT linear measurements combined with clinical factors can discriminate between AD patients and healthy aged controls. Among a series of linear measurements, temporal horn ratio and suprasellar cistern ratio, which reflect MTA, most significantly contributed to the discriminations. Considering the simplicity and practicality of linear measurements as well as the inexpensiveness and availability of CT, these linear measurements could be of value in evaluating brain atrophy in work-up of AD patients.

5.2 PAPER 2

5.2.1 CSF biomarkers

Our observation of significantly increased concentration of CSF T-tau and P-tau protein, as well as decreased Aβ42 in AD patients is in line with that of previous studies [103]. Our finding that P-tau was not significantly increased in AD patients with CVC compared with healthy aged controls, suggests that CVC increase the variability of P-tau protein accumulation in AD patients.

5.2.2 The relations between CSF biomarkers and brain atrophy

Only a few studies have investigated the cross-sectional relations between CSF biomarkers and brain atrophy assessments [24, 81-83]. Regarding CSF tau, two studies from De Leon et al [24, 83] found that P-tau correlated with hippocampal volume in MCI. A correlation between P-tau231 and baseline hippocampal volume in AD was presented in a study by Hampel et al [104]. Furthermore, two studies reported significant correlations between Aβ42 and temporal lobe atrophy [105] as well as between Aβ42 and whole brain atrophy [106]. Recently it has been suggested that CSF and MRI markers independently contribute to the diagnosis of AD, since no correlation was found between them [81]. The differences in selection of subjects and the various assessments of brain atrophy could contribute to the reported discrepancies [81]. We have also considered another possible reason for the discrepancies, which is the presence of CVC in AD patients. Therefore, we calculated correlations between the CSF biomarkers and the linear measurements in pure AD, AD+CVC, and the control group separately.

In this study, the CSF biomarkers correlated with many measurements of brain atrophy in pure AD patients. This result supports the view that the CSF biomarkers are related to brain atrophy and indicate the progressive pathological changes in AD. The finding of a correlation between P-tau protein and MTA is in line with the conclusion

of De Leon et al. [24, 83] It is also shown here that P-tau and MTA dependently contribute to the diagnosis of AD, which is contradictory to the results of the study by Niki et al [81].

When AD is accompanied by CVC, however, we found only significant correlation between P-tau and Evans ratio (E/C) which typically reflects central atrophy and frontal lobe atrophy. Most of the correlations between the CSF biomarkers and brain atrophy that are evident in pure AD patients disappeared when CVC were presented among the AD subjects. One possible explanation is that CVC affect the pattern of atrophy process in AD, over and above age and AD itself. The influence of CVC on brain atrophy in AD results in a loss of dependency between the CSF biomarkers and atrophy. As mentioned above, the other possibility is that CVC could also affect the accumulation of CSF biomarkers in AD. This could be an important explanation for the conflicting results in the literature, since it has most often not taken the presence of CVC into account. Moreover, to some extent, it might also explain the diversity of the pathological progression of clinically diagnosed AD.

In healthy aged controls, T-tau correlated to cella media index (G/A), which is a typical measurement to indicate enlargement of lateral ventricle body, or central atrophy. This finding suggests that T-tau could be an indicator of general and widespread damage to brain tissue and might not be specific for AD.

5.2.3 The combined use of markers of brain atrophy and CSF

Consequently, it may be of value to separate AD+CVC from pure AD, when evaluating the contribution of the CSF biomarkers and brain atrophy assessments to the diagnosis of AD. The discriminant analyses in this study showed that the combined use of markers of brain atrophy and CSF biomarkers did not increase the accuracy of classification of pure AD from the controls. On the other hand, in AD patients with CVC, the combined use of the two markers increased the number of correctly classified patients, mostly depending on an increased specificity. This could be of value in selecting more effective tools in the diagnosis of AD. If subjects assumed to have AD are ascertained to have CVC by clinical CT examination, the combined use of CSF biomarkers and MTA assessment (CT linear measurement: temporal horn ratio) will help increase the accuracy of the diagnosis of AD. If the clinical subjects do not have CVC, it is not necessary to use the MTA assessment combined with CSF biomarkers (Fig. P2-2). The finding suggests that it might be important for a radiologist to also report minor cerebrovascular damage on CT or MRI images, even in patients suspected of having AD.
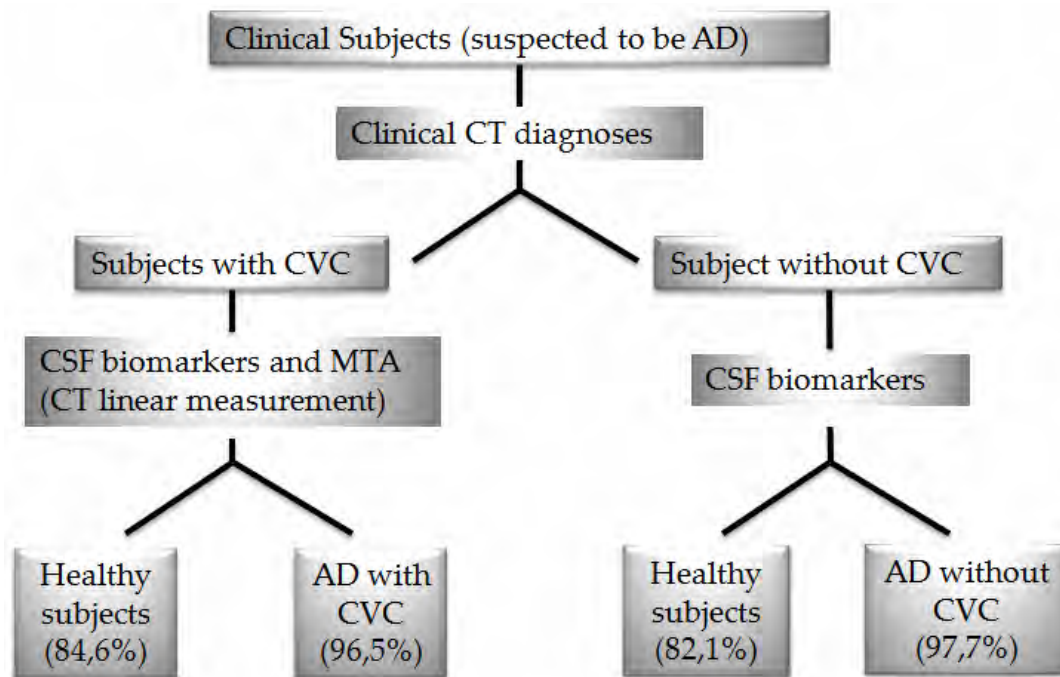
Fig. P2-2. If clinical subjects that are suspected of having AD are ascertained to have CVC by clinical CT examination, the combined use of CSF biomarkers and MTA assessment is useful to increase the accuracy of the diagnosis of AD. If the clinical subjects do not have CVC, it is not necessary to use the MTA assessment combined with CSF biomarkers. (The percentages of correct classification in this figure are from the results in Table3.)

5.2.4 The most important factor - Aβ42

In the discriminant analyses, Aβ42 was the most important factor in the diagnosis of AD (with or without CVC). Our study supports the view that the alteration of the amyloidogenic pathway plays a major pathogenic role [107, 108], even if CVC are present in AD.

5.2.5 Study limitation of the CT studies

One limitation of this study is whether linear measurements of brain atrophy are effective enough to reflect manifold brain atrophy. On the other hand, since some of the volumetric assessments of brain atrophy in MRI lack acknowledged accuracy, and it is especially hard for general raters (non-radiologist) to deal with the anatomic variations in individual brains, a simple and reliable linear measurement could reflect more accuracy in some specific atrophy and it would be easy to manage. Linear measurement could be a tool for estimating brain atrophy in AD, and could be used not only in CT, but also in MRI images. However, more studies are needed to clarify how the different types and degrees of CVC affect brain atrophy and the CSF biomarkers in AD.

MRI is more sensitive than CT in detecting CVC and can be used for visual rating and volume measurements of CVC. Therefore, one other issue regarding this study is whether the assessments of CVC by CT were reliable enough in establishing the presence of CVC.

5.2.6 Conclusions of Paper 2

In conclusion, P-tau correlates with the linear radiological measurement of MTA only in pure AD without CVC. Combined with the linear measurement of MTA, the diagnostic value of CSF biomarkers, especially specificity, can be increased, but only in AD with CVC. The linear measurements of MTA are of value in AD diagnosis.

5.3 PAPER 3

5.3.1 The natural status of age-related brain atrophy

Along with the development of higher quality MRI images and volumetric methods, we described again the natural status of age-related brain atrophy in a large sample of non-demented elderly individuals. We focused on gender differences and lateral symmetry of hippocampus and ventricular size in order to better understand the diversity of volumetric studies in the literature. The diversity, which could be due to different selection of samples, different age ranges, protocols of delineations, quality of images, and controlling for ICV or not [47], obscures the understanding of hippocampus shrinkage in normal aging. In this population-based study, the large number of subjects and the carefully selected protocol of delineation should make it possible to obtain a more valid assessment of the status of age-related brain atrophy.

5.3.1.1 Head size

The very large individual variance of head size and the significant gender differences implies that it is really necessary that the brain volumes are adjusted or normalized by head size in analyses. This has been used more and more widely in studies.

5.3.1.2 Expansion of ventricles

Expansion of ventricles represents central atrophy, which might in part be induced by silent cerebrovascular changes in subcortical and peri-ventricular areas in the elderly. Such cerebrovascular changes might be an important component of cerebral degeneration. The large variation of ventricle size found in our study might suggest large variance in distribution and progression of silent cerebrovascular lesions in a non-demented elderly population.

5.3.1.3 Lateral asymmetry

It has been argued that atrophy in the left hippocampus is more severe than that in the right in AD patients and therefore more vulnerable to AD pathology [29-31]. In the non-demented sample of this study, however, the left hippocampus was generally smaller than the right. The finding that lateral asymmetry of hippocampus has been the natural status in non-demented elderly, rather than a result of AD pathology, may be seen as against the notion that left hippocampus is more vulnerable for AD. A larger right cerebral hemisphere has also been seen in relatively young adults [48]. This may imply that already in young adults the right hippocampus is larger than the left, but this needs to be proved by further studies with young subjects.

5.3.1.4   Gender differences

The males in this study showed bigger ventricles and smaller hippocampus than the females. This finding is in line with other studies showing similar gender difference [41, 47]. However, this does not prove that elderly males have more severe brain atrophy. To identify whether males or females have more rapid atrophy, the rate of volume loss in longitudinal studies or the rate of AAT in cross-sectional studies must firstly be considered. Concerning the rate of AAT in this study, the atrophy of hippocampus in females was faster than that in males, regardless of the inclusion or exclusion of the oldest subsamples. Our finding is consistent with that in two previous studies [40, 41], supporting the view that females are more vulnerable to hippocampus atrophy than males, even if the males generally demonstrated smaller hippocampus than the females, which might have already existed in early adulthood. To confirm this, further studies including younger adult are needed.

5.3.2   The important factors in brain atrophy - age and gender

The conclusions that age and gender are important factors in brain atrophy [38, 109] are confirmed in our study. Though education is related to AD [110], it made no contribution to hippocampus atrophy and the expansion of ventricles in our sample.

5.3.3   Dramatic brain volume changes between 81 and 84 years

Dramatic volume changes of brain structures in the two oldest age groups were observed (Figure 3). The expansion of ventricles demonstrated reversal after 81years, especially in males. The size of hippocampus was increased between 81y-84y and decreased again after 84y. This could be due to a possible increase in mortality or morbidity of dementia around 81y-84y, and less atrophy in the surviving or non-demented very aged elderly persons in our study. Therefore, care should be taken in interpreting results when very old subjects are included in volumetric studies. A small sample size in very aged groups could also influence the results.

5.3.4   Acceleration of hippocampal atrophy

In addition to estimating the rate of AAT, we conducted a large number of regression analyses to find out the age point at which acceleration of total hippocampal atrophy starts. These analyses identified this point of acceleration as being 72 years of age. For expansion of the ventricles, no such acceleration in atrophy was found. The finding that acceleration of hippocampal atrophy is present among healthy aged subjects must be further evaluated in longitudinal studies. From this data we cannot exclude the effect of selection-bias in the older groups. The alternative might be that the accelerated hippocampal atrophy could be due to pre-clinical AD pathology striking the medial temporal lobe.

The selection of discontinuous ages in the subjects is one limitation of the study. Somewhere between 70-75 years, instead of 72 years old, might better represent the age when the acceleration of hippocampus atrophy starts. A continuous age range would make it possible to more precisely study the age point at which atrophy acceleration starts. To clarify the full progression of brain atrophy in life span, younger subjects also need to be included in future studies.

5.3.5 Conclusions of Paper 3

In conclusion, the males had smaller hippocampal volumes (normalized by ICV) than females; however, the females were more vulnerable to hippocampal atrophy in a non-demented elderly population. An acceleration of hippocampal atrophy may emerge and start around 72 years of age in non-demented elderly population.

5.4 PAPER 4

5.4.1 Vascular factors and brain atrophy

In this community-based MRI study of cognitively intact older people, we found that: (1) current smoking, binge alcohol intake and high total cholesterol were associated with a smaller volume of hippocampus – the associations were more evident among men, whereas diabetes was related to a reduced volume of entorhinal cortex; (2) an increasing burden of vascular risk factors was related to the reduced volumes of hippocampus and entorhinal cortex, especially among men; (3) a higher MMSE score was associated with larger volumes of both hippocampus and entorhinal cortex; and (4) physical activity, hypertension, BMI, and a history of coronary heart disease did not significantly affect the volumes of hippocampus and entorhinal cortex. These findings suggest that vascular factors, especially increasing burden of multiple vascular factors, may be involved in the degenerative process of the brain aging.

5.4.2 Study limitation

This is a population-based MRI study with a relatively large sample. The assessments on vascular factors and disorders were rather comprehensive. However, some limitations related to the cross-sectional design deserve mentioning. Firstly, selective survival related to vascular factors and diseases (e.g., smoking, hypertension, coronary heart disease, and diabetes) might have led to the observed cross-sectional association towards null. Secondly, there may be a potential for selection bias because the subjects included in the analysis may be healthier than those not included. Finally, findings from this Nordic group may not be generalizable to other ethnic groups such as Asians and African-Americans because volumetric measures of the brain and prevalence of vascular factors and diseases vary substantially among various ethnic and racial groups [84].

In the Washington-Heights-Inwood Columbia Aging Project of multi-ethnic older people, a history of vascular disease (e.g., hypertension, diabetes, and heart disease) was associated with a smaller relative brain volume, but was not associated with hippocampal volume nor with entorhinal volume [84].

5.5 GENERAL SUMMARY OF CONCLUSIONS

The simple CT linear measurements (temporal horn ratio and suprasellar cistern ratio) combined with clinical factors can discriminate between AD patients and healthy aged controls. Combined with the linear measurement of MTA, the diagnostic value of CSF biomarkers, especially specificity, can be increased, but only in AD with CVC. The females were more vulnerable to hippocampal atrophy in a non-demented elderly population. An acceleration of hippocampal atrophy may emerge and start around 72 years of age in non-demented elderly population. An increasing burden of vascular risk factors was related to the reduced volumes of hippocampus and entorhinal cortex, especially among men.

5.6 FUTURE ASPECTS

More mature methods to evaluate brain atrophy, more comprehensive investigations of brain atrophy in full range of age and more meticulous studies concerning anatomical variations may be the key aspects in the future exploration of brain atrophy.

6 ACKNOWLEDGEMENTS

In the last several years, as a researcher, I have been in the process of finishing my thesis, a period during which I have experienced both the happiness of bringing my talent and imagination into full play, and the puzzlement of exploring. Many persons around me, supervisors, colleagues, cooperators and friends, kindly and generously helped me in their own unique ways, which has constituted innumerable important elements in the completion of this thesis. Those moments have been saved in my memory with lots of Mb as protected documents. Now I would like to open them again to read them from the heart.

Lars-Olof Wahlund, my first supervisor, guided the direction of my research. He gave me a great deal of freedom and plenty of time to think and try, making it possible for me to bring my imagination and exploration fully into play. He showed tolerance and patience in listening to many of my novel ideas, though not always scientific, and to accept that I often disturbed him outside his working calendar just for a brief discussion or a fast decision. I am most fortunate that he is my supervisor.

Peter Aspelin, my co-supervisor, is a great boss always doing a lot of "business". We regularly sit around his big oval table, on which there is always a wooden hammer owned by the chairman of the Swedish Radiological Association. With his great leadership, he made sure that my research was always on the right track, and particularly, kept the writings and revisions of our manuscripts going well within the time schedule and the logical framework.

Lena Bronge, my co-supervisor, is a senior radiological medical doctor. She helped correct the papers in every detail using her professional knowledge and patience.

Laura Fratiglioni, recommended me to Lars-Olof at the beginning, guided me and cooperated with me in the big SNAC-K national project. She also shared the pleasure with me in Montreal when I won the 2nd place of the International Phychogeratrical Association Junior Prize.

Here I would like also to thank **Helena Forssell** for being so helpful in handling a large number of documents for me, so that I could feel relaxed all the time; and to thank **Anette Eidehall** for patiently and regularly answering my question "where is Lars-Olof?". And my colleagues and co-workers, I would like to mention their names for accompanying and testifying my work: **Olof**, **Eric**, *Teacher* **Zhu**, **Qiu**; the hospital physicists who took care of "Bidlab" from the beginning until now: **Daggi**, **Eva-Lena**, **Lisa, and Eva**; and the program "terminator" **Leif**.

"Bildlab", in the beginning with only one user - me, and now with many users, is the place where I spent most of my working time and I will miss it. With more and more computers and updated software, the temperature and noise appeared to increase every day. The space on the hard disk never seems to be able to catch up with the accumulation of the data. Listening to music via a headset while working with images that I used to do to keep noise away has become a routine for all of the users in Bidlab. Especially, my closest colleague, Olof likes to listen to classical operas or even more so classic historic e-novels. This may represent some of his character, which makes him the unique person that has discussed the anatomic complexities of the brain with me.

52

7 REFERENCES

1. Marksteiner, J., H. Hinterhuber, and C. Humpel, *Cerebrospinal fluid biomarkers for diagnosis of Alzheimer's disease: beta-amyloid(1-42), tau, phospho-tau-181 and total protein.* Drugs Today (Barc), 2007. **43**(6): p. 423-31.
2. Thompson, P.M., et al., *Tracking Alzheimer's disease.* Ann N Y Acad Sci, 2007. **1097**: p. 183-214.
3. Jorm, A.F., A.E. Korten, and A.S. Henderson, *The prevalence of dementia: a quantitative integration of the literature.* Acta Psychiatr Scand, 1987. **76**(5): p. 465-79.
4. McKhann, G., et al., *Clinical diagnosis of Alzheimer's disease: report of the NINCDS-ADRDA Work Group under the auspices of Department of Health and Human Services Task Force on Alzheimer's Disease.* Neurology, 1984. **34**(7): p. 939-44.
5. Blacker, D., et al., *Reliability and validity of NINCDS-ADRDA criteria for Alzheimer's disease. The National Institute of Mental Health Genetics Initiative.* Arch Neurol, 1994. **51**(12): p. 1198-204.
6. *Association, A.P., Diagnostic and Statistical Manual of Mental disorders, 4th Edition Text Revision. 2000, Washington DC.*
7. Dubois, B., et al., *Research criteria for the diagnosis of Alzheimer's disease: revising the NINCDS-ADRDA criteria.* Lancet Neurol, 2007. **6**(8): p. 734-46.
8. Hampel, H., et al., *Core candidate neurochemical and imaging biomarkers of Alzheimer's disease.* Alzheimers Dement, 2008. **4**(1): p. 38-48.
9. Braak, E., et al., *Neuropathology of Alzheimer's disease: what is new since A. Alzheimer?* Eur Arch Psychiatry Clin Neurosci, 1999. **249 Suppl 3**: p. 14-22.
10. Laakso, M.P., et al., *Volumes of hippocampus, amygdala and frontal lobes in the MRI-based diagnosis of early Alzheimer's disease: correlation with memory functions.* J Neural Transm Park Dis Dement Sect, 1995. **9**(1): p. 73-86.
11. Seab, J.P., et al., *Quantitative NMR measurements of hippocampal atrophy in Alzheimer's disease.* Magn Reson Med, 1988. **8**(2): p. 200-8.
12. Kesslak, J.P., O. Nalcioglu, and C.W. Cotman, *Quantification of magnetic resonance scans for hippocampal and parahippocampal atrophy in Alzheimer's disease.* Neurology, 1991. **41**(1): p. 51-4.
13. Jack, C.R., Jr., et al., *MR-based hippocampal volumetry in the diagnosis of Alzheimer's disease.* Neurology, 1992. **42**(1): p. 183-8.
14. Soininen, H., M. Puranen, and P.J. Riekkinen, *Computed tomography findings in senile dementia and normal aging.* J Neurol Neurosurg Psychiatry, 1982. **45**(1): p. 50-4.
15. Braak, H. and E. Braak, *Staging of Alzheimer-related cortical destruction.* Int Psychogeriatr, 1997. **9 Suppl 1**: p. 257-61; discussion 269-72.
16. Braak, H. and E. Braak, *Neuropathological stageing of Alzheimer-related changes.* Acta Neuropathol, 1991. **82**(4): p. 239-59.
17. Gomez-Isla, T., et al., *Profound loss of layer II entorhinal cortex neurons occurs in very mild Alzheimer's disease.* J Neurosci, 1996. **16**(14): p. 4491-500.
18. Thompson, P.M., et al., *Dynamics of gray matter loss in Alzheimer's disease.* J Neurosci, 2003. **23**(3): p. 994-1005.
19. Dickerson, B.C., et al., *MRI-derived entorhinal and hippocampal atrophy in incipient and very mild Alzheimer's disease.* Neurobiol Aging, 2001. **22**(5): p. 747-54.
20. Frisoni, G.B., et al., *Hippocampal and entorhinal cortex atrophy in frontotemporal dementia and Alzheimer's disease.* Neurology, 1999. **52**(1): p. 91-100.
21. Laakso, M.P., et al., *MRI of the hippocampus in Alzheimer's disease: sensitivity, specificity, and analysis of the incorrectly classified subjects.* Neurobiol Aging, 1998. **19**(1): p. 23-31.

22. Laakso, M.P., et al., *Hippocampal volumes in Alzheimer's disease, Parkinson's disease with and without dementia, and in vascular dementia: An MRI study.* Neurology, 1996. **46**(3): p. 678-81.
23. Thompson, P.M., et al., *Mapping hippocampal and ventricular change in Alzheimer disease.* Neuroimage, 2004. **22**(4): p. 1754-66.
24. de Leon, M.J., et al., *MRI and CSF studies in the early diagnosis of Alzheimer's disease.* J Intern Med, 2004. **256**(3): p. 205-23.
25. Wahlund, L.O., et al., *Visual rating and volumetry of the medial temporal lobe on magnetic resonance imaging in dementia: a comparative study.* J Neurol Neurosurg Psychiatry, 2000. **69**(5): p. 630-5.
26. Callen, D.J., et al., *Beyond the hippocampus: MRI volumetry confirms widespread limbic atrophy in AD.* Neurology, 2001. **57**(9): p. 1669-74.
27. Du, A.T., et al., *Magnetic resonance imaging of the entorhinal cortex and hippocampus in mild cognitive impairment and Alzheimer's disease.* J Neurol Neurosurg Psychiatry, 2001. **71**(4): p. 441-7.
28. De Santi, S., et al., *Hippocampal formation glucose metabolism and volume losses in MCI and AD.* Neurobiol Aging, 2001. **22**(4): p. 529-39.
29. Barnes, L.L., et al., *Sex differences in the clinical manifestations of Alzheimer disease pathology.* Arch Gen Psychiatry, 2005. **62**(6): p. 685-91.
30. Nitrini, R., et al., *Mortality from dementia in a community-dwelling Brazilian population.* Int J Geriatr Psychiatry, 2005. **20**(3): p. 247-53.
31. Di Carlo, A., et al., *Incidence of dementia, Alzheimer's disease, and vascular dementia in Italy. The ILSA Study.* J Am Geriatr Soc, 2002. **50**(1): p. 41-8.
32. Muller, M.J., et al., *Functional implications of hippocampal volume and diffusivity in mild cognitive impairment.* Neuroimage, 2005. **28**(4): p. 1033-42.
33. Pennanen, C., et al., *Hippocampus and entorhinal cortex in mild cognitive impairment and early AD.* Neurobiol Aging, 2004. **25**(3): p. 303-10.
34. Convit, A., et al., *Specific hippocampal volume reductions in individuals at risk for Alzheimer's disease.* Neurobiol Aging, 1997. **18**(2): p. 131-8.
35. Jack, C.R., Jr., et al., *Rates of hippocampal atrophy correlate with change in clinical status in aging and AD.* Neurology, 2000. **55**(4): p. 484-89.
36. Wu, C.C., et al., *Brain structure and cognition in a community sample of elderly Latinos.* Neurology, 2002. **59**(3): p. 383-91.
37. Convit, A., et al., *Age-related changes in brain: I. Magnetic resonance imaging measures of temporal lobe volumes in normal subjects.* Psychiatr Q, 1995. **66**(4): p. 343-55.
38. Tang, Y., et al., *Brain volume changes on longitudinal magnetic resonance imaging in normal older people.* J Neuroimaging, 2001. **11**(4): p. 393-400.
39. Coffey, C.E., et al., *Quantitative cerebral anatomy of the aging human brain: a cross-sectional study using magnetic resonance imaging.* Neurology, 1992. **42**(3 Pt 1): p. 527-36.
40. Lupien, S.J., et al., *Hippocampal volume is as variable in young as in older adults: implications for the notion of hippocampal atrophy in humans.* Neuroimage, 2007. **34**(2): p. 479-85.
41. Pruessner, J.C., et al., *Age and gender predict volume decline in the anterior and posterior hippocampus in early adulthood.* J Neurosci, 2001. **21**(1): p. 194-200.
42. Jernigan, T.L. and A.C. Gamst, *Changes in volume with age--consistency and interpretation of observed effects.* Neurobiol Aging, 2005. **26**(9): p. 1271-4; discussion 1275-8.
43. Raz, N., et al., *Regional brain changes in aging healthy adults: general trends, individual differences and modifiers.* Cereb Cortex, 2005. **15**(11): p. 1676-89.
44. Raz, N., et al., *Differential aging of the medial temporal lobe: a study of a five-year change.* Neurology, 2004. **62**(3): p. 433-8.
45. Walhovd, K.B., et al., *Effects of age on volumes of cortex, white matter and subcortical structures.* Neurobiol Aging, 2005. **26**(9): p. 1261-70; discussion 1275-8.
46. Dekaban, A.S., *Changes in brain weights during the span of human life: relation of brain weights to body heights and body weights.* Ann Neurol, 1978. **4**(4): p. 345-56.

47. Coffey, C.E., et al., *Sex differences in brain aging: a quantitative magnetic resonance imaging study.* Arch Neurol, 1998. **55**(2): p. 169-79.

48. Carne, R.P., et al., *Cerebral cortex: an MRI-based study of volume and variance with age and sex.* J Clin Neurosci, 2006. **13**(1): p. 60-72.

49. Jobst, K.A., L.P. Barnetson, and B.J. Shepstone, *Accurate prediction of histologically confirmed Alzheimer's disease and the differential diagnosis of dementia: the use of NINCDS-ADRDA and DSM-III-R criteria, SPECT, X-ray CT, and APO E4 medial temporal lobe dementias. The Oxford Project to Investigate Memory and Aging.* Int Psychogeriatr, 1997. **9 Suppl 1**: p. 191-222; discussion 247-52.

50. Wahlund, L.O., et al., *White matter hyperintensities in dementia: does it matter?* Magn Reson Imaging, 1994. **12**(3): p. 387-94.

51. Lopez, O.L., et al., *Computed tomography--but not magnetic resonance imaging--identified periventricular white-matter lesions predict symptomatic cerebrovascular disease in probable Alzheimer's disease.* Arch Neurol, 1995. **52**(7): p. 659-64.

52. Giesel, F.L., et al., *Temporal horn index and volume of medial temporal lobe atrophy using a new semiautomated method for rapid and precise assessment.* AJNR Am J Neuroradiol, 2006. **27**(7): p. 1454-8.

53. Pedersen, N.L., et al., *Neuroimaging findings in twins discordant for Alzheimer's disease.* Dement Geriatr Cogn Disord, 1999. **10**(1): p. 51-8.

54. Hasuda, K., et al., *Afferent loop obstruction diagnosed by sonography and computed tomography.* Br J Radiol, 1991. **64**(768): p. 1156-8.

55. Weinberger, D.R., et al., *Computed tomography in schizophreniform disorder and other acute psychiatric disorders.* Arch Gen Psychiatry, 1982. **39**(7): p. 778-83.

56. Sabattini, L., *Evaluation and measurement of the normal ventricular and subarachnoid spaces by CT.* Neuroradiology, 1982. **23**(1): p. 1-5.

57. Synek, V. and J.R. Reuben, *The ventricular-brain ratio using planimetric measurement of EMI scans.* Br J Radiol, 1976. **49**(579): p. 233-7.

58. Scheltens, P., et al., *The diagnostic value of magnetic resonance imaging and technetium 99m-HMPAO single-photon-emission computed tomography for the diagnosis of Alzheimer disease in a community-dwelling elderly population.* Alzheimer Dis Assoc Disord, 1997. **11**(2): p. 63-70.

59. Jack, C.R., Jr., et al., *Prediction of AD with MRI-based hippocampal volume in mild cognitive impairment.* Neurology, 1999. **52**(7): p. 1397-403.

60. Wang, P.N., et al., *Prediction of Alzheimer's disease in mild cognitive impairment: a prospective study in Taiwan.* Neurobiol Aging, 2006. **27**(12): p. 1797-806.

61. Jack, C.R., Jr., et al., *Rate of medial temporal lobe atrophy in typical aging and Alzheimer's disease.* Neurology, 1998. **51**(4): p. 993-9.

62. Laakso, M.P., et al., *Hippocampus in Alzheimer's disease: a 3-year follow-up MRI study.* Biol Psychiatry, 2000. **47**(6): p. 557-61.

63. Krasuski, J.S., et al., *Volumes of medial temporal lobe structures in patients with Alzheimer's disease and mild cognitive impairment (and in healthy controls).* Biol Psychiatry, 1998. **43**(1): p. 60-8.

64. Teipel, S.J., et al., *Comprehensive dissection of the medial temporal lobe in AD: measurement of hippocampus, amygdala, entorhinal, perirhinal and parahippocampal cortices using MRI.* J Neurol, 2006. **253**(6): p. 794-800.

65. Xu, Y., et al., *Usefulness of MRI measures of entorhinal cortex versus hippocampus in AD.* Neurology, 2000. **54**(9): p. 1760-7.

66. Ashburner, J. and K.J. Friston, *Voxel-based morphometry--the methods.* Neuroimage, 2000. **11**(6 Pt 1): p. 805-21.

67. Baron, J.C., et al., *In vivo mapping of gray matter loss with voxel-based morphometry in mild Alzheimer's disease.* Neuroimage, 2001. **14**(2): p. 298-309.

68. Busatto, G.F., et al., *A voxel-based morphometry study of temporal lobe gray matter reductions in Alzheimer's disease.* Neurobiol Aging, 2003. **24**(2): p. 221-31.

69. Teipel, S.J., et al., *Multivariate deformation-based analysis of brain atrophy to predict Alzheimer's disease in mild cognitive impairment.* Neuroimage, 2007. **38**(1): p. 13-24.

70. Lerch, J.P., et al., *Focal decline of cortical thickness in Alzheimer's disease identified by computational neuroanatomy.* Cereb Cortex, 2005. **15**(7): p. 995-1001.

71. Lerch, J.P., et al., *Automated cortical thickness measurements from MRI can accurately separate Alzheimer's patients from normal elderly controls.* Neurobiol Aging, 2008. **29**(1): p. 23-30.

72. Stefani, A., et al., *AD with subcortical white matter lesions and vascular dementia: CSF markers for differential diagnosis.* J Neurol Sci, 2005. **237**(1-2): p. 83-8.

73. Hampel, H., et al., *Core biological marker candidates of Alzheimer's disease - perspectives for diagnosis, prediction of outcome and reflection of biological activity.* J Neural Transm, 2004. **111**(3): p. 247-72.

74. Hulstaert, F., et al., *Improved discrimination of AD patients using beta-amyloid(1-42) and tau levels in CSF.* Neurology, 1999. **52**(8): p. 1555-62.

75. Ikeda, S., et al., *Evidence of amyloid beta-protein immunoreactive early plaque lesions in Down's syndrome brains.* Lab Invest, 1989. **61**(1): p. 133-7.

76. Haass, C., et al., *Amyloid beta-peptide is produced by cultured cells during normal metabolism.* Nature, 1992. **359**(6393): p. 322-5.

77. Strozyk, D., et al., *CSF Abeta 42 levels correlate with amyloid-neuropathology in a population-based autopsy study.* Neurology, 2003. **60**(4): p. 652-6.

78. Spillantini, M.G., et al., *Topographical relationship between beta-amyloid and tau protein epitopes in tangle-bearing cells in Alzheimer disease.* Proc Natl Acad Sci U S A, 1990. **87**(10): p. 3952-6.

79. Buerger, K., et al., *Differential diagnosis of Alzheimer disease with cerebrospinal fluid levels of tau protein phosphorylated at threonine 231.* Arch Neurol, 2002. **59**(8): p. 1267-72.

80. Frankfort, S.V., et al., *Amyloid beta protein and tau in cerebrospinal fluid and plasma as biomarkers for dementia: a review of recent literature.* Curr Clin Pharmacol, 2008. **3**(2): p. 123-31.

81. Schoonenboom, N.S., et al., *CSF and MRI markers independently contribute to the diagnosis of Alzheimer's disease.* Neurobiol Aging, 2008. **29**(5): p. 669-75.

82. Wahlund, L.O. and K. Blennow, *Cerebrospinal fluid biomarkers for disease stage and intensity in cognitively impaired patients.* Neurosci Lett, 2003. **339**(2): p. 99-102.

83. de Leon, M.J., et al., *Longitudinal CSF and MRI biomarkers improve the diagnosis of mild cognitive impairment.* Neurobiol Aging, 2006. **27**(3): p. 394-401.

84. Brickman, A.M., et al., *Brain morphology in older African Americans, Caribbean Hispanics, and whites from northern Manhattan.* Arch Neurol, 2008. **65**(8): p. 1053-61.

85. Raz, N., et al., *Neuroanatomical correlates of fluid intelligence in healthy adults and persons with vascular risk factors.* Cereb Cortex, 2008. **18**(3): p. 718-26.

86. Folstein, M.F., S.E. Folstein, and P.R. McHugh, *"Mini-mental state". A practical method for grading the cognitive state of patients for the clinician.* J Psychiatr Res, 1975. **12**(3): p. 189-98.

87. Mohs, R.C., W.G. Rosen, and K.L. Davis, *The Alzheimer's disease assessment scale: an instrument for assessing treatment efficacy.* Psychopharmacol Bull, 1983. **19**(3): p. 448-50.

88. Blennow, K., et al., *Tau protein in cerebrospinal fluid: a biochemical marker for axonal degeneration in Alzheimer disease?* Mol Chem Neuropathol, 1995. **26**(3): p. 231-45.

89. Vanmechelen, E., et al., *Quantification of tau phosphorylated at threonine 181 in human cerebrospinal fluid: a sandwich ELISA with a synthetic phosphopeptide for standardization.* Neurosci Lett, 2000. **285**(1): p. 49-52.

90. Andreasen, N., et al., *Cerebrospinal fluid beta-amyloid(1-42) in Alzheimer disease: differences between early- and late-onset Alzheimer disease and stability during the course of disease.* Arch Neurol, 1999. **56**(6): p. 673-80.
91. Aylward, E.H., et al., *Suprasellar cistern measures as a reflection of dementia in Alzheimer's disease but not Huntington's disease.* J Psychiatr Res, 1991. **25**(1-2): p. 31-47.
92. Meese, W., et al., *CT evaluation of the CSF spaces of healthy persons.* Neuroradiology, 1980. **19**(3): p. 131-6.
93. Gomori, J.M., et al., *The assessment of changes in brain volume using combined linear measurements. A CT-scan study.* Neuroradiology, 1984. **26**(1): p. 21-4.
94. Starkstein, S.E., et al., *Brain atrophy in Huntington's disease. A CT-scan study.* Neuroradiology, 1989. **31**(2): p. 156-9.
95. Hamano, K., et al., *A comparative study of linear measurement of the brain and three-dimensional measurement of brain volume using CT scans.* Pediatr Radiol, 1993. **23**(3): p. 165-8.
96. Pascual-Leone, A., A. Dhuna, and D.C. Anderson, *Cerebral atrophy in habitual cocaine abusers: a planimetric CT study.* Neurology, 1991. **41**(1): p. 34-8.
97. Sheline, Y.I., et al., *Stereological MRI volumetry of the frontal lobe.* Psychiatry Res, 1996. **67**(3): p. 203-14.
98. Pantel, J., et al., *A new method for the in vivo volumetric measurement of the human hippocampus with high neuroanatomical accuracy.* Hippocampus, 2000. **10**(6): p. 752-8.
99. Jutila, L., et al., *MR volumetry of the entorhinal, perirhinal, and temporopolar cortices in drug-refractory temporal lobe epilepsy.* AJNR Am J Neuroradiol, 2001. **22**(8): p. 1490-501.
100. Insausti, R., et al., *MR volumetric analysis of the human entorhinal, perirhinal, and temporopolar cortices.* AJNR Am J Neuroradiol, 1998. **19**(4): p. 659-71.
101. Pino, A., et al., *Discriminant analysis to study trace elements in biomonitoring: an application on neurodegenerative diseases.* Ann Ist Super Sanita, 2005. **41**(2): p. 223-8.
102. Maruyama, K., S. Ikeda, and N. Yanagisawa, *[Correlative study of the brain CT and clinical features of patients with Down's syndrome in three clinical stages of Alzheimer type dementia].* Rinsho Shinkeigaku, 1995. **35**(7): p. 775-80.
103. Blennow, K. and H. Hampel, *CSF markers for incipient Alzheimer's disease.* Lancet Neurol, 2003. **2**(10): p. 605-13.
104. Hampel, H., et al., *Correlation of cerebrospinal fluid levels of tau protein phosphorylated at threonine 231 with rates of hippocampal atrophy in Alzheimer disease.* Arch Neurol, 2005. **62**(5): p. 770-3.
105. Schroder, J., et al., *Cerebral changes and cerebrospinal fluid beta-amyloid in Alzheimer's disease: a study with quantitative magnetic resonance imaging.* Mol Psychiatry, 1997. **2**(6): p. 505-7.
106. Hansson, O., et al., *Association between CSF biomarkers and incipient Alzheimer's disease in patients with mild cognitive impairment: a follow-up study.* Lancet Neurol, 2006. **5**(3): p. 228-34.
107. Oddo, S., et al., *Triple-transgenic model of Alzheimer's disease with plaques and tangles: intracellular Abeta and synaptic dysfunction.* Neuron, 2003. **39**(3): p. 409-21.
108. Selkoe, D.J. and D. Schenk, *Alzheimer's disease: molecular understanding predicts amyloid-based therapeutics.* Annu Rev Pharmacol Toxicol, 2003. **43**: p. 545-84.
109. Raz, N., et al., *Aging, sexual dimorphism, and hemispheric asymmetry of the cerebral cortex: replicability of regional differences in volume.* Neurobiol Aging, 2004. **25**(3): p. 377-96.
110. Paradise, M., C. Cooper, and G. Livingston, *Systematic review of the effect of education on survival in Alzheimer's disease.* Int Psychogeriatr, 2009. **21**(1): p. 25-32.